IEEE Access
Multidisciplinary ⋮ Rapid Review ⋮ Open Access Journal

Received 17 July 2025, accepted 8 August 2025, date of publication 18 August 2025, date of current version 27 August 2025.

Digital Object Identifier 10.1109/ACCESS.2025.3599744

SURVEY

Advances in Receiver and Detection Systems for Low Earth Orbit Nanosatellite Quantum Communications

JAMES J. SHAWE, JERRY HORGAN, AND DEIRDRE KILBANE
Walton Institute for Information and Communication Systems Science, SETU West Campus, Waterford, X91 P20H Ireland

Corresponding author: James J. Shawe (james.shawe@waltoninstitute.ie)

This publication has emanated from research conducted with the financial support of Taighde Éireann-Research Ireland under Grant number 13/RC/2077_P2 at CONNECT: the Research Ireland Centre for Future Networks. This publication has also emanated from research supported in part by the South East Regional Development (SERD) fund.

ABSTRACT Satellite quantum communications have received a surge of interest in recent years, encouraged by the success of the QUESS experiments and as a reaction to advances in quantum computing. This work focuses on low Earth orbit nanosatellite missions, which offer several benefits (e.g. lower costs, greater launch availability, easier to replenish) over satellites at different orbit heights (medium Earth orbit, geosynchronous Earth orbit) and satellite size classes (e.g. small-sats, etc). Recent work on low Earth orbit satellite Quantum Key Distribution (QKD) has focused on transmitters and quantum sources, with less attention paid to the receiver side of the link. This review addresses that imbalance by focusing on the receiver and detection systems of satellite quantum communications. This work has found that two-way beacon acquisition and tracking systems are both a common element of state-of-the-art missions, and likely to remain a critical subsystem to ensure high-quality satellite-to-ground station links; however, improvements to detection and tracking algorithms could be made. For discrete variable QKD, receivers and detection systems in nanosatellites at low Earth orbit are likely to remain using silicon single photon avalanche diodes, while receivers and detection systems in optical ground stations may opt for superconducting nanowire single photon detectors, as cryogenic cooling is feasible. For continuous variable QKD, the receivers and detection systems, using coherent detection systems, share many hardware elements with classical optical satellite communications. Combined with coherent detection systems' inherent resilience to operating during daytime conditions, this makes continuous variable QKD an attractive prospect for future missions, if its fundamental challenges can be overcome.

INDEX TERMS Nanosatellite quantum communications, QKD, quantum communications, LEO nanosatellite communications, DV-QKD, CV-QKD.

I. INTRODUCTION

Satellite quantum communications is a rapidly growing research topic. The field has garnered interest for applications in remote clock synchronisation, deep space communications, metrology, sensing, distributed and secure multi-party computing, entangled interferometric imaging arrays with remote telescopes for astronomy, and for its provably secure communications via quantum key distribution (QKD) [1].

The associate editor coordinating the review of this manuscript and approving it for publication was Peng-Yong Kong.

QKD represents the most mature quantum communication application with several decades of heritage, culminating in multiple Discrete Variable (DV) and Continuous Variable (CV) protocols using either prepare and measure or entanglement distribution schemes. As such, the implementation of QKD via the emerging technology of satellite quantum communications can be seen as a logical stepping stone, after which other applications will benefit and follow. The advances of quantum computing may pose a security threat, both in the future where quantum computing may be ubiquitous, and now by storing stolen sensitive data and

decrypting it later when quantum computing is available. QKD offers security based on the laws of quantum mechanics and is set to become the new backbone for all encryption, replacing the classical paradigm of security based on computational difficulty. Increasing the scope beyond security, the infrastructure can support entanglement distribution, which will lead to advanced applications of satellite quantum communications that depend on it, and thus, lead to the quantum internet.

The goal of all QKD systems is to maximise the number of secret keys that can distributed in a given timeframe, and this requirement is passed onto the receivers and detection systems of these QKD systems.

In the current literature on satellite quantum communications, the focus has been dominated by transmitters and sources. This paper aims to address the lack of attention to receivers and detection systems. Previous reviews on this topic have been quite broad, with less focus on Low Earth Orbit (LEO) nanosatellite missions, and the receiver and detection systems of those missions [2]. Other reviews on similar, overlapping topics have mentioned the focus of this work in brief [3]. This review differs from previous reviews by its focus on receiver and detection systems for LEO nanosatellite missions, either ground station or satellite-based. Some small-sat missions have been included either for reference or as the technology is also applicable to nanosatellites. Several of the common challenges surrounding LEO nanosatellite quantum communications are highlighted in this work, along with current state-of-the-art implementations of technology overcoming them. The main contributions of this paper are:

- Catalogues the current state-of-the-art LEO nanosatellite quantum communication receivers and detection systems whose performance has been experimentally demonstrated in the lab or demonstrated through mission deployment.
- Discusses the challenges and limitations of the current state-of-the-art components consisting of the receiver and detection system.
- Suggests several solutions and future directions of improvement, particularly in regards to combining both classical optical satellite communication hardware and quantum satellite communication hardware.

The rest of the paper is organised as follows: Subsection I-A outlines the research methodology of the study. subsection I-C discusses several of the system-wide challenges facing satellite quantum communications. Subsection I-D provides a direct comparison with classical optical satellite communications, to clearly distinguish the unique elements of quantum satellite communications from the aspects that are common between both. Section II describes the current state-of-the-art Acquisition, Tracking, and Pointing (ATP) systems and the challenges facing them. Section III discusses the current state-of-the-art for the receiver subsystem and again follows with an analysis of several of the challenges surrounding it. Section IV then discusses the current state-of-the-art detection systems and associated challenges. Finally, in Section V, several conclusions are drawn.

A. RESEARCH METHODOLOGY

Papers were collected under the following selection criteria:

- Papers detailing LEO nanosatellite missions with receivers and detection systems are no older than five years.
- Papers that detail seminal satellite quantum communications missions, like QUESS, are included for reference.
- Papers older than five years that include technology that is still relevant or used in the previously selected papers are included for reference.
- Papers which reported experimental results from technology demonstration missions, laboratory experiments, or active mission deployment were given greater importance.
- Review papers were selected when they covered overlapping topics relevant to this work.

This work defines the overall receiver and detection system as a composite of three main subsystems, whether as an Optical Ground Station (OGS) or satellite receiver. These subsystems are:

- **Receiver**. The receiver optics are defined, for this work, as the components responsible for guiding the signal to the detectors and, if using two-way beacon guides, separating the beacon signal. This subsystem is important as compromised, dirty, and/or misaligned optics can disrupt the quantum signal creating signal loss.
- **Acquisition, Tracking, and Pointing (ATP)**. Alternatively called Pointing, Acquisition, and Tracking (PAT), ATP systems are required to ensure accurate alignment of the optical axes of the OGS and the satellite (or between both satellites, in the case of inter-satellite links). Adaptive Optics (AO) systems are also included within this definition, as they are often integrated with the ATP system, although they are more critical for correcting wavefront corruption due to atmospheric effects. The ATP system is vital to LEO nanosatellite quantum communications as loss of tracking can cause signal loss, reducing the rate at which secret keys can be distributed.
- **Detection system**. This work defines the detection system as the primary mechanism for registering a received signal. Different types of detection systems will be explored later in the work. This subsystem is critical to LEO nanosatellite quantum communications, as incorrectly setup or compromised detection systems can severely reduce the amount of valid detections, and thus reduce the secret key rate of quantum communications.

B. NANOSATELLITE FOCUS

This work focuses on advances in receivers and detection systems used mainly in nanosatellite missions in LEO, and the generalised receiver and detection systems illustrated in the figures are based on the advances of those nanosatellite missions. These generalised receivers and detection systems intrinsically hold specific considerations regarding optical performance for nanosatellites in LEO. However, some aspects could be extrapolated generally to other satellite classes. A prominent distinction between a nanosatellite and a small satellite is the maximum aperture size of the telescope that can be installed, with small-sats able to use much larger apertures. Additionally, control over the pointing errors of an APT system must be more stringent for nanosatellites than for small-sats, as the larger the aperture on the satellite, the more resilient the overall link gain is to pointing errors [4]. Thus, the ability of the APT systems discussed in this work to maintain low pointing errors is likely to be a specific consideration for nanosatellites.

C. NANOSATELLITE QUANTUM COMMUNICATION CHALLENGES

There are two central contributors to the challenges and limitations of nanosatellite quantum communications. One is photon loss in the channel, which scales exponentially with channel length; especially true for entangled photon sources [5]. The other is false detections arising from dark counts from the detectors themselves or from background noise in the form of stray light. A core characteristic of quantum mechanics that gives QKD its edge in security is also one of the biggest challenges to its implementation. The no-cloning theorem ensures that the quantum signal cannot be amplified, which thus puts pressure on the receiver and detection system to discriminate accurately the weak attenuated transmitted signal from the many sources of background noise. A short, non-exhaustive summary of the contributors to channel loss and false detection events (accurate at least for signal frequencies between 20 THz, or 14,990 nm, and 375 THz, or 800 nm) is given:

- **Diffraction.** The spreading of the transmitted quantum signal due to diffraction.
- **Turbulence.** This causes regions of changing refractive index in the atmosphere, which can cause wavefront aberrations and/or deflect light as it passes through. It is responsible for scintillation effects, which are devastating to phase-dependent protocols like Continuous Variable QKD (CV-QKD).
- **Atmospheric losses.** This is defined as the losses due to the absorption and scattering of light as it passes through the atmosphere. It is only relevant for the dense regions of the atmosphere up to 20 km above the ground, past which the particle density is much lower.
- **Pointing errors.** These are errors that occur due to the receiver and transmitter hardware operating with imprecise tracking.
- **Detection efficiency.** All detectors have an innate efficiency or quantum efficiency, which is wavelength-dependent and represents the detectors' ability to successfully register an event when all other losses are negligible.
- **Optics efficiency.** There is some associated loss whenever light passes through optics due to absorption, or from imperfect transmissivity and reflection.
- **Dark counts.** These are counts that are registered on the detector even though no event has occurred. This can be measured by covering the detector from light and measuring the counts per second to derive the dark count rate. Cooling can typically reduce this rate.
- **Background light.** This is defined as any unwanted light that enters the system, creating background noise for the detection system.
- **Polarisation basis errors.** This is due to the misalignment of transmitted and received polarisation bases. Unless corrected, this is disastrous for QKD protocols that rely on the polarisation to encode the key.
- **Phase errors.** Similar to polarisation basis errors, this arises from a misalignment of the transmitted phase of the signal and the received phase of the signal. For coherent detection (such as detectors used in CV-QKD), this is often fatal unless it can be corrected. Scintillation is often a large contributor to phase mismatch.
- **Doppler shift.** This is a significant challenge for coherent communications (like CV-QKD), For LEO satellites, transmitting at 1566 nm wavelength, the Doppler shift can be in the range of around $\pm$ 4.2 GHz at 400 km with a rate of change of 90 MHz/s and $\pm$ 4.5 GHz at 600 km with a rate of change of 56 MHz/s [6].
- **Sensitivity to noise.** In a QKD protocol, the presence of a third-party eavesdropper is deduced from excessive noise in the channel. The security of the protocol relies on the noise level in the channel being kept below a threshold, and as noise due to attenuation or other disruptive effects will be indistinguishable from errors generated by a third-party eavesdropper, satellite quantum communications are extremely sensitive to noise.

The cumulative effect on a light signal from atmospheric losses, turbulence, and pointing errors is angular spreading, spatial spreading, temporal spreading and transmission loss, which ultimately results in a loss in signal amplitude, an increase in background noise, and fluctuations in the received amplitude and phase [7].

D. COMPARISON WITH CLASSICAL OPTICAL SATELLITE COMMUNICATIONS

There are many similarities between both LEO nanosatellite quantum communications and LEO nanosatellite classical optical communications in regards to both the challenges they face (as outlined in Subsection I-C) and the technology that is used to overcome them; specifically the ATP systems, aspects

of the receivers, and coherent detection systems (detailed in Sections II, III, and IV-A2).

In classical optical satellite communication, receivers utilise photodetectors to convert incoming light into electrical signals for data extraction, emphasising high data rates and operational simplicity. This is typically achieved by either Intensity Modulated Direct Detection (IM-DD) modulation (like On-Off-Keying (OOK)) where a signal is registered by the generation of an electric pulse from a direct impact of a photon, or by a coherent system modulation (like Phase Shift Keying (PSK)) where a signal is registered through differences in phase, frequency and/or polarisation by coherent detection.

In contrast, satellite quantum communication, typically under a discrete variable QKD protocol, employs single-photon detectors, like Single-Photon Avalanche Detectors (SPADs) or Superconducting Nanowire Single-Photon Detectors (SNSPDs), to detect individual photons and measure their quantum states. Under a CV-QKD protocol, satellite quantum communications will typically employ coherent detection. In terms of hardware, the receiver and detection system may be identical to the coherent detection systems of classical optical satellite communication. The key differences between the classical and quantum systems under this protocol is that a Quantum Random Number Generator (QRNG) will determine the random symbols to be modulated and transmitted, rather than modulating a typical data stream like in a classical system, and that basis selection on both the transmitter and receiver is also typically determined by a QRNG. Satellite quantum communications also involve unique post-processing procedures like basis sifting, shot noise unit calibration, and privacy amplification. Some post-processing procedures, typically implemented through Digital Signal Processing (DSP) (like demultiplexing, clock synchronisation, and downsampling), can be used in both coherent classical optical satellite communications and satellite quantum communications.

Additionally, another key difference between classical optical coherent communications and quantum coherent communications lies in the definition of heterodyne detection. For a classical heterodyne detection system, the reference signal has a fixed offset in frequency and phase to the modulated signal, even when the signal contains null information. To extract the encoded information, the two signals are compared by mixing the reference and modulated signal and measuring them with a Positive-Intrinsic-Negative (PIN) photodiode. Given that the reference and modulated signal are constant in frequency and optical power, a beat note will characterise the resulting superposition of the two with an amplitude proportional to the product of the two electric field amplitudes. It is the beat note that is analysed to extract the encoded information, and by carefully selecting the offset between the reference and modulated signal, the beat frequency can be chosen to be in the radio or microwave band to be easily processed by electronics after photodiode detection. For quantum communications, heterodyne detection is also known as dual-homodyne detection, as the Local Oscillator (LO) and the modulated signal, of the same frequency, are sent to two different homodyne detectors, which allows measurement of orthogonal phase components simultaneously; thus at the cost of increased complexity, the phase estimation is enhanced [8]. Most literature for quantum communications will refer to this definition of heterodyne detection, including this work.

There are several common challenges (and common solutions) that face both classical optical and quantum satellite communications systems utilising LEO nanosatellite platforms, including those addressed in Section II on ATP systems (except AO systems) and those addressed in Section III on receivers. Detection systems for both tend to be unique in the challenges faced, strategy, and implementation. Although, as discussed previously, there is overlap in coherent detection systems that could be exploited.

Summarising generally, classical systems prioritise speed and ease of implementation, with less importance on errors in the channel as signals can be amplified and repeated to improve link quality. Quantum systems focus on security, which is based on a determined threshold tolerance to errors in the channel, and the integrity of quantum information, which is integral due to the inability to replicate quantum states. These two separate design philosophies are reflected in the receiver and detection systems of both.

E. ORBITAL ALTITUDE

The selected orbit of satellite quantum communications typically falls into one of three broad categories, ordered by increasing altitude: LEO, Medium Earth Orbit (MEO), and Geostationary Earth Orbit (GEO). This work exclusively addresses nanosatellites in LEO conditions; however, the impact of higher-altitude orbits, such as MEO and GEO, on the receiver and detection systems and strategies of quantum satellite communications should not be understated or overlooked.

Previous literature has utilised the Priandola-Laurenza-Ottaviani-Banchi (PLOB) bound [9], [10] to estimate the secret key rate between a ground station and a satellite at various altitudes, including the effects of diffraction, extinction and quantum efficiency [11]. The theoretical model assumed a collimated Gaussian beam at 800 nm wavelength with a beam waist of 20 cm, a receiver aperture size of 40 cm, and a detection efficiency of 0.4. The resulting performance showed a high Secret Key Rate (SKR) for LEO and a usable SKR for MEO. However, orbital dynamics must be considered for LEO and MEO, which will further reduce the SKR.

In general, LEO and GEO have been identified as the most suitable for satellite QKD, due to their respective strengths, with MEO receiving less interest due to challenges arising from its intermediate position between LEO and GEO [2]. LEO has a significant strength with its relative proximity between transmitter and receiver, but has a weakness in

high speeds that present a challenge to the ATP system, and introduce Doppler shift effects to the signal. Additionally, LEO communication windows will be limited to typically around five minutes for each pass, requiring efficient use of QKD protocols. The advantages for GEO are both the capability for continuous operation of QKD due to its stationary position relative to Earth, and its large coverage [12]. It can also use a minimal tracking system (compared to LEO), and doesn't require accounting for the Doppler shift. The disadvantages of GEO are higher losses due to the distance between the transmitter and receiver, and higher associated costs with launching a satellite to GEO. MEO has a balance of both these advantages and disadvantages.

II. ACQUISITION, TRACKING, AND POINTING

ATP systems are vital to enabling the precision links required for LEO nanosatellite QKD, which must overcome high angular speeds and whose errors can have a significant impact on the viable communication time. The errors for tracking systems are typically expressed as the Root-Mean-Square Error (RMSE). Fine-pointing requirements are derived from the detector's active area. For example, given a detector active area of $200 \times 200\ \mu m^2$, the RMSE of the fine pointing system must be $\pm 100 \mu$m or smaller. As stated in Section I-A, AO systems are defined as part of the ATP system for this work, but typically have slightly different objectives. While an ATP system aims to acquire, track and point towards the incoming signal, AO systems correct wavefront aberrations, assisting the ATP system, but more critically enabling fibre coupling to detection systems and/or preserving important qualities of the quantum signal.

A. ADAPTIVE OPTICS

AO systems correct for wavefront errors in laser beam propagation that arise due to atmospheric turbulence. Although AO was originally used for astronomy, it has been widely adopted today to improve the efficiency of coupling quantum signals into ground terminal fibre for satellite quantum communication. A Fast Steering Mirror (FSM) compensates for tip-tilt deformations to the beacon beam, while a Deformable Mirror (DM) compensates for high-order wavefront errors.

Work has been done to integrate AO and quantum communication systems [13]. The authors transmitted a 780 nm polarisation-based weak coherent pulse for qubits and co-propagated this with an 808 nm laser beacon (with a timing pulse 40 ns ahead of the qubits) to probe atmospheric turbulence and compensate with the AO system. This field experiment demonstrated that higher-order AO greatly increased the quantum channel efficiencies by combining AO, spectral, spatial and temporal filtering through a 1.6 km horizontal path, which emulated downlink propagation through atmospheric turbulence for daylight satellite QKD.

Quantum optical setups differ from classical AO systems in several key aspects. AO systems of classical optical communication setups typically seek to maximise data throughput and signal quality, focusing on achieving high Signal-to-Noise Ratios (SNR) and low Bit Error Rates (BER), as seen in demonstrations of pre-compensation AO systems [14]. Precompensation or pre-distortion techniques, where the signal is purposely corrupted by the AO system before transmission so that atmospheric effects restore the signal before being detected, have become an active area of research [14], [15]. AO systems are used to improve link quality by minimising scintillation effects and stability by minimising dropouts, which will result in error correction and retransmission events increasing overhead. The loss of some photons (a decrease in long-term average power) is not as important.

For quantum communication setups, the role of an AO system is to tightly focus the signal at the receiver to increase the total number of measured photons; this is much more important than signal fluctuations over short timescales, as each photon will contribute to the protocol [16]. The AO system for quantum communications favours increasing the long-term averaged power (total number of measured photons), despite potential short-term power variance increases from bursts and dropouts. Increasing the total number of photons measured typically increases the throughput of QKD protocols, and any increases to the link budget via AO systems can significantly boost secret key generation rates [16]. Additionally, classical optical systems tend to be more tolerant of minor wavefront errors, but quantum setups require much more precise wavefront correction as seen in literature [17].

A generalised AO system is illustrated in Figure 1. AO systems are mandatory for efficient coupling to Single-Mode Fibre (SMF) and thus the detection systems that rely on SMF connections (e.g. SNSPDs). Additionally, AO systems are useful for preserving quantum signal information, like that encoded in phase. As discussed, both classical optical and quantum satellite communications benefit from an AO system, with classical communication missions such as the National Aeronautics and Space Administration's (NASA) TeraByte Infrared Delivery (TBIRD) mission demonstrating its effectiveness for SMF coupling in a LEO nanosatellite mission [18]. Additionally, SMF coupling efficiency improvements were demonstrated to increase the secret key rate in quantum communication setups using an AO system [17]. An OGS connected to the terrestrial Croatian Quantum Communication Infrastructure, using an AO system to couple the received quantum signal to SNSPDs, has been proposed [19].

In a general AO system loop, the wavefront of an incoming signal is measured by a Shack-Hartmann wavefront sensor, whose output is sent to a Real-Time Computer (RTC) or Field Programmable Gate Array (FPGA). An algorithm then computes the optimal position of each element of the deformable mirror and outputs them, typically as voltages, to the deformable mirror, which then adjusts accordingly. The speed at which this loop completes is defined as the Closed-Loop Control Bandwidth (CLCB). It has been shown

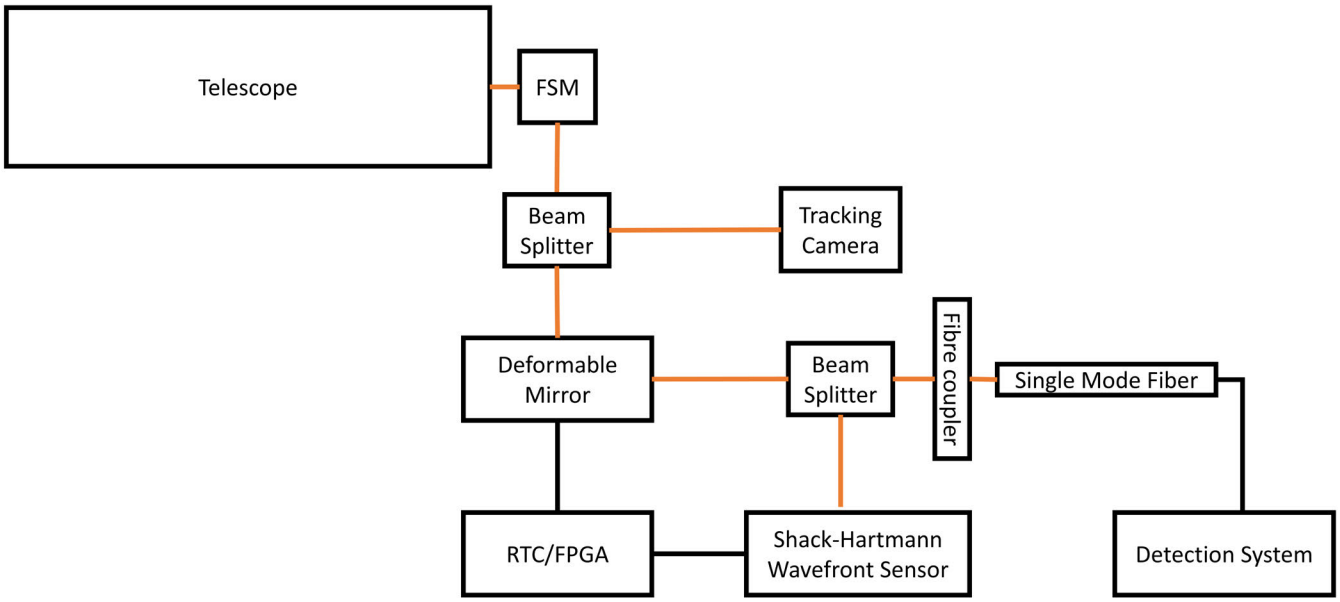

FIGURE 1. A general adaptive optics configuration.

that AO systems can increase resilience to stronger and faster varying turbulence by increasing the number of elements in the system and/or by increasing the CLCB until it is at least higher than the Greenwood frequency to achieve good coupling performance [20], [21], [22]. It can be expected that improvements to the CLCB could be made from faster, more advanced and more efficient control algorithms that compute optimal updates to the deformable mirror's actuators, or by computing on faster or more efficient hardware, and/or with machine learning predictive models for the wavefront sensor.

LEO nanosatellite QKD transmitters present a challenge to AO systems, as corrections in the deformable mirror tend to lag behind the optical path of the signal. For a solution, recent work has shown that adding a pioneer beacon, spatially separated from the signal at the transmitter by some distance (1 to 5 m), can reduce the anisoplanatism of the AO correction for wavelength division multiplexing schemes; with the best results emerging from a novel spatial multiplexing system for optical terminals capable of distinguishing the two beams simultaneously [23].

Adaptive optics systems are often cost-prohibitive. An exciting area of research is investigating whether machine learning can be used to replace the Shack-Hartmann wavefront sensor that is typically seen in AO systems. Under particular conditions, a reinforcement learning algorithm achieved a performance close to 90% of a Shack–Hartmann wavefront sensor-based AO system [24]. Even at a worse performance, if adequate for the high requirements for quantum communications, it may be a feasible alternative. Nevertheless, increased research may match or even exceed the performance of Shack-Hartmann wavefront sensor AO systems and reduce the cost of the AO system overall.

B. ADVANCES IN ATP SYSTEMS

ATP systems for nanosatellites are largely similar for both classical optical communications and quantum communications. There has been a large focus on improving the performance of ATP systems in classical optical naosatellite communications, particularly for intersatellite regimes. This work is limited to downlink and uplink connections and includes some of the advancements seen in ATP systems for classical optical communications due to these systems' compatibility with quantum communications.

Research within the **German Aerospace Centre's (DLR) OSIRIS program** has experimented with various ATP systems on LEO satellites, including: open-loop downlinks without optomechanical pointing mechanisms [25], and closed-loop body pointing with and without independent beam steering [26]. Research of ATP systems in LEO nanosatellites began with OSIRISv4CubeSat, utilising active beam steering and body pointing, achieved with a quadrant photodiode as a sensor and a FSM as an actuator to steer the beam [27]. Future LEO nanosatellite research is built on OSIRISv4CubeSat with QUBE, a mission focused on performing QKD experiments [27], [28].

The **QSpace team**, in anticipation of a full QKD link between a LEO nanosatellite and the Zvenigorod Observatory OGS, developed the Vector payload to test critical systems, including the ATP system and polarisation reference-frame synchronisation. The Vector payload, designed for classical optical satellite communications, is a 2.5U full duplex optical terminal with an expected bit rate of 50 Mbps at 808 nm uplink and 850 nm downlink; using a Silicon Photomultiplier (SPiM) for a receiver on the nanosatellite [29]. The ATP protocol begins with open loop coarse tracking by using ephemeris data, until the 525 nm satellite beacon is received

by the wide Field Of View (FOV) 70 mm coarse camera attached to the barrel of the main aperture; at which point coarse closed-loop tracking begins and takes over control of the alt-azimuth mount which slews to follow the satellite [30]. The beacon and signal, now acquired by the main aperture, are then guided by a FSM to a dichroic mirror separating them. A beam splitter then splits the now separate beacon, reflecting one branch to a narrow FOV Complementary Metal-Oxide-Semiconductor (CMOS) 640 × 640 100 Hz fine pointing camera, and combined with a controller for the FSM, completes the fine pointing closed control loop [30]. On the nanosatellite side, a wide FOV camera is used to detect the 671 nm OGS beacon, which then controls a FSM to correct for misalignment in a closed-loop system. The results of these tests on the ATP system are to be incorporated into the full QKD mission. Full details of the final design of the mission and spacecraft are still in active development; however, operations are expected to be performed in nighttime conditions [29].

The typically weak quantum signal associated with LEO satellite quantum communications results in stringent pointing accuracy requirements for ATP systems. The **QUESS mission** launched the Micius small-sat with an entangled photon quantum source, and entangled photons cannot be amplified, so to optimise the link efficiency, the beam divergence was kept narrow and close to the diffraction-limited far-field divergence angle (12 μrad) [5], [31]. The narrow divergence angle necessitated strict pointing and tracking requirements, which were addressed with a two-way laser beacon system. The OGS 671 nm beacon was transmitted to Micius and acquired first by a coarse camera attached to a scanning head, in a closed control loop with a two-axis turntable system, with a range of ± 90° azimuth and -30° to 75° elevation in the satellite body frame for reference [5], [31]. The control error was less than 50 μrad with a bandwidth greater than 3 Hz [31]. After coarse tracking, the beacon was guided to the piezoelectric ceramic actuator-based FSM, in turn directing it to the fine tracking camera and closing the second control loop [31]. The satellite 532 nm beacon was received by OGSs with an identical ATP system, and all links were performed in nighttime conditions [5], [31].

QEYSSat, an upcoming quantum communications small-sat designed to perform QKD over uplink, used a two-way beacon ATP system with a Beacon Laser Assembly (BLA) consisting of three fibre launchers with individual tip/tilt control and fixed divergence angles of 0.74°in its field-testing of the satellite receiver using an aeroplane and mobile OGS to simulate LEO passes [32]. A BLA was mounted upon the telescope of both the ground transmitter and the satellite receiver and fed 850 nm laser light from a fibre-coupled Beacon Laser Source (BLS) array [32]. The receiving beacon laser cameras were 2 megapixels, 50 fps imaging cameras with an 850 nm bandpass filter of width 10 nm, mounted to the telescopes [32]. Initial acquisition was achieved by transmitting Global Positioning System (GPS) positional data (longitude, latitude) and altitude as measured by the Inertial Navigation Module (INM) over a classical RF link [32]. The INM had an attitude uncertainty (± 2.5°) larger than that of the beam divergence of the beacons, which necessitated the attachment of an additional Light Emitting Diode (LED) with a large beam divergence (around 80°) to the satellite receiver [32]. This LED was switched on before beacon acquisition and turned off once the OGS beacon was detected by the receiver's beacon camera [32]. A Commercial Off The Shelf (COTS) two-axis motor system facilitated coarse pointing of the ATP system, driven by a custom algorithm that minimised beacon spot deviation from a calibrated reference position on the camera's detector by taking into account three factors: the estimated angular speed calculated from position differences between frames, the spot's current deviation and the accumulated spot deviations [32]. After coarse pointing, both beacon and quantum signal were guided by an FSM into the satellite's Fine Pointing Unit (FPU), within which they were separated by a dichroic mirror, with the beacon directed to a quad cell photo-sensor that informed a fine-pointing controller and completed the closed loop with the FSM [32]. These results were obtained exclusively in nighttime conditions, with daytime conditions not attempted [32].

The **Mount Stromlo optical communication ground station** is designed to support the Artemis program as a lunar communication receiver and quantum communication detection [33]. Its ATP system is similar to the designs previously discussed: initial acquisition is achieved with ephemeris data combined with a coarse pointing closed control loop attached to a 20 arcminute FOV guide telescope mounted to the barrel of the main telescope [33]. The coarse pointing system uses a 512 × 640 cooled InGaAs camera for satellite beacon detection with a filter to eliminate solar background [33]. The ground station beacon is transmitted by a laser launch telescope mounted to the barrel of the main receiver telescope, able to transmit beacon lasers at 1064 nm and 1550 nm and maintain a point ahead angle for LEO communication [33].

ROKS uses a two-way beacon system for its LEO nanosatellite QKD downlink mission, enabled by the APATITE APT module of the nanosatellite. A unique trait of the APATITE module is that instead of a predetermined reference coordinate on the CMOS sensor, an alignment laser, generated in the quantum source module JADE, is spatially coupled with the quantum signal through SMF connecting JADE with APATITE and is used to determine accurate pointing and tracking [34]. The alignment beam and quantum signal are separated in the APATITE module by dichroic mirrors, with the alignment laser directed towards the CMOS sensor and the quantum signal spatially coupled with the downlink beacon generated in APATITE [34]. A Micro-Electromechanical System (MEMS) mirror is used to align the uplink beacon, the quantum source, and the downlink beacon. The alignment beam spot on the CMOS sensor becomes the reference spot with which the closed-loop

TABLE 1. Advances in ATP systems and suggested improvements.

Advances in ATP systems	Suggested improvements to ATP systems
Miniaturisation of space systems from small-sat to nanosatellite platforms [34]. Satellite telescopes have utilised Schmidt-Cassegrain designs for compactness and wider, useful field of view [34]. Implemented a point-ahead algorithm and ATP system to account for the Earth's rotation and beacon laser offset [31]. Alternative beacon spot detection algorithms such as corner detection, have been demonstrated in labs [35]. Alternative beacon tracking algorithms such as optical flow, have been demonstrated in labs [35]. An Alignment Laser has been used instead of a reference coordinate on a CMOS sensor [34]. Downlink beacon wavelengths in the 780-850 nm range have been used on a satellite, while uplink beacon wavelengths in the 1520-1600 nm have been used in OGSs [32]–[34].	Improved beacon spot detection algorithms, minimising loop time for calculations. Improved beacon tracking algorithms, minimising loop time for calculations. Increased cycles of beacon camera sensors to minimise background noise, enabled by faster loop times from better algorithms.

MEMS mirror controller will aim to align the uplink beacon spot. An offset between the overlapping beacon spots can be created to implement point-ahead algorithms [34]. ROKS, and its ATP system, is designed to be operational in nighttime conditions [34].

A summary of the advances and suggested improvements is given in Table 1.

C. ATP SYSTEMS CHALLENGES AND LIMITATIONS

Several challenges and limitations of the ATP systems for LEO nanosatellite quantum communications are discussed. An effective ATP system includes several prerequisites: suitable actuators for the telescope mount capable of providing both accuracy and speed to keep the beacons of the ATP system aligned under the high slew rates encountered in LEO communications, and the ability to calculate new positions efficiently and quickly to control the mount and point it at the satellite or OGS accurately. A visualisation of the suggested improvements and/or areas that could benefit from optimisation for current ATP systems is given in Fig. 2.

1) POINT AHEAD ANGLE

The point ahead angle is a dynamically calculated factor that is required in downlink configurations to overcome both the beacon offset from the receiving aperture (if the beacon is launched in a guide telescope separate from the main receiving aperture), and the relative motion of the OGS to the satellite due to the angular rotation of the Earth, as they are two of the biggest contributors to the pointing error in the downlink channel [31]. In uplink configurations, these contributions are not as large and can be reasonably ignored [31]. The QUESS mission solved this by offsetting the fine tracking point of the received beacon to compensate. The control algorithm of the FSM was designed to calculate the required offset from a reference point on the CMOS sensor that ensured the transmission and reception optical axes were offset during the pass, creating the point ahead angle [31].

The control algorithm was implemented on a 32-bit floating point digital signal processor and given the satellite position, velocity, and attitude in real-time, directly from the onboard GPS and Attitude and Orbit Determination, and Control System (AODCS), along with the OGS position uploaded before or at any point in operations [31]. The algorithm calculated a coordinate on the CMOS sensor and passed it to the FPGA controller as a reference input. The beacon spot position was detected on the CMOS sensor of the fine tracking camera, using the grey centroid algorithm, and the FPGA controller then directed the FSM to move the beacon spot to the reference spot, completing the loop [31]. The point ahead angle is dynamic as the tracking point is calculated throughout the satellite's pass over an OGS.

2) BACKGROUND LIGHT AND DAYTIME OPERATIONS

A significant challenge to beacon recognition and tracking is background light on the detector, which obfuscates the beacon spot. It can be suppressed by increasing the sampling frequency of the sensor or by reducing the filter bandwidth of the optical system [35]. The corner detection method for beam spot detection in individual frames, combined with the optical flow method to calculate the displacement of the beam spot between frames has been used for ATP system tracking, matching the accuracy of the grey centroid method and taking a total processing time of 0.75 ms on an FPGA [35]. Given this, it is reasonable to deduce that faster beacon spot detection algorithms and tracking algorithms will enable faster calculation loop times and improve performance in the presence of background light.

Acquisition, tracking and pointing during daytime conditions are particularly challenging due to the high intensity of background light from all wavelengths emitted by the Sun. Operations in nighttime conditions remain the most popular option for LEO nanosatellite QKD missions, as discussed in several of the missions reviewed in this work [5], [29], [32], [34]. This is in no small part due to the difficulty in detecting the beacon signal and maintaining accurate pointing and tracking in the presence of excessive background light. Careful selection of beacon wavelength (discussed shortly) and filtering may enable daytime operations for the traditional two-way beacon system common in this review. However, NASA's TBIRD mission performed its experiments

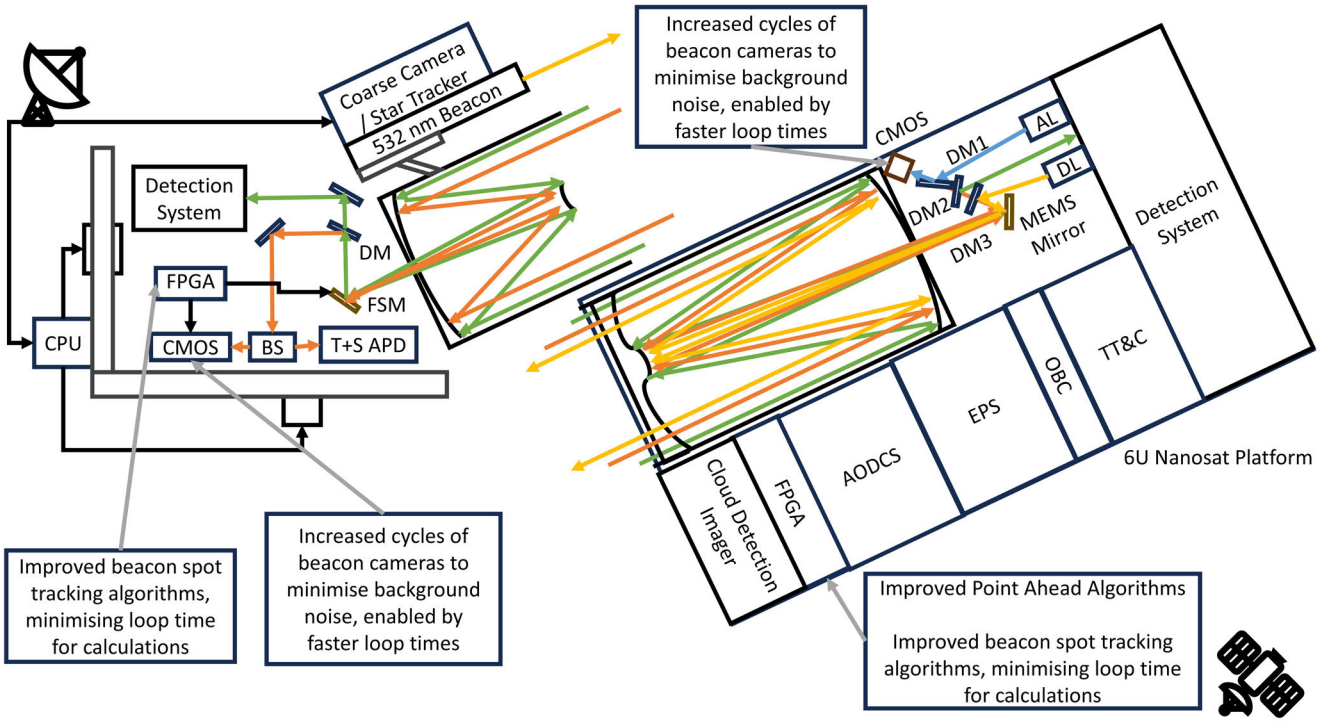

FIGURE 2. Suggested improvements of ATP systems for OGSs and satellites. The quantum signal is denoted by green. Beacon Tx, in the receiver frame of reference, is denoted by yellow. Beacon Rx, in the receiver frame of reference, is denoted by red. The alignment laser is denoted by light blue. Power/Data lines are denoted by black.

in both daytime and nighttime conditions, demonstrating that coherent communications can be used for ATP systems to enable tracking in daytime conditions [18]. Further discussion is provided in Section III-B.

3) WEATHER EFFECTS

Weather effects can also have a significant impact on the performance of an ATP system, including obstruction of the beacon signals by clouds or aerosols, which will effectively block all tracking and result in the loss of the signal. Weather effects also significantly impact the quantum signal detection, and further discussion is provided in Section III-B.

4) OPTICAL MISALIGNMENT

Optical misalignment in satellites can arise from violent launch vibrations and environmental effects from space, like thermal displacement, which results in permanent biases in alignment, as observed in the QUESS mission [31]. The challenge of optical misalignment can be more difficult to solve for nanosatellite platforms, where redundancy and fail-safes are often discarded. The alignment laser from the ROKS nanosatellite overcomes the issue by aligning the incoming uplink signal with the alignment laser, overlapping the signals on the CMOS sensor, and removing the need to use a reference coordinate on a CMOS sensor [34]. The alignment laser and the quantum signal are spatially coupled and frequency multiplexed, so this technique should, in principle, make the system robust to any permanent biases that may arise during launch and operations.

5) NANOSATELLITE MICROVIBRATIONS

Micro-vibrations on a nanosatellite platform, arising from any source of mechanical movement like reaction wheels in the AODCS, will introduce pointing jitter to the system. Motorised half-wave plates have been used onboard the Galassia nanosatellite during its technology demonstration of Spontaneous Parametric Down Conversion (SPDC) production with a Barium Borate (BBO) crystal [36]. For quantum communication receivers onboard nanosatellites, they could be used to correct polarisation drift, as the QUESS mission used them in their OGS [5]. Vibration and jitter will be introduced to the nanosatellite platform through the motorisation and, in combination with other sources, could present a significant challenge to the ATP system.

Liquid Crystal Devices (LCD) have been successfully used to manipulate the polarisation state of light for basis selection in QKD, where Liquid Crystal Retarders (LCR) are combined with two Quarter-Wave Plates (QWP) and a Polarising Beam Splitter (PBS) to create a Liquid Crystal Polarisation Rotator (LCPR) [37]. LCDs use low amounts of power, are lightweight and compact, have a fast response time, do not contain moving parts, and have been used in onboard nanosatellites. SpooQy-1, a 3U nanosatellite polarisation entangled quantum source technology demonstrator, uses

LCPRs instead of motorised wave plates, as part of its polarisation analyser before the detectors [38]. The use of LCDs over motorised wave plates on a LEO nanosatellite receiver could solve the challenge of microvibrations to the ATP system. However, a strong temperature dependence and performance drift present a challenge when using LCDs, but both can be overcome by capacitance tracking and recalibration [37].

6) BEACON WAVELENGTH

The choice of wavelength for a beacon typically requires a trade-off between considerations of background noise, atmospheric attenuation, detector efficiency, and, to a lesser extent, the cost and availability, for any particular wavelength [39]. Classical optical LEO nanosatellite communication systems typically use wavelengths between 780-850 nm or 1520-1600 nm for beacons and signal transmission, as there is a good balance between these factors, however, 1550 nm is the most widely adopted range for data transmission and is less harmful to human eyesight than shorter wavelengths [39]. Beacons are less sensitive to detector efficiency than quantum signals, as they can be amplified to improve link quality. Thus, beacons and data transmission in classical channels at 1550 nm for LEO nanosatellite QKD missions is a reasonable choice. There has been a range of beacon wavelengths in QKD satellite missions, however, as discussed previously in Section II-B.

7) DETECTOR CHOICE

The choice of beacon detector typically hinges on the optimum FOV. In general, a wide FOV detector is beneficial to aid faster beacon acquisition; however, a larger FOV will introduce more background noise to the system, while a smaller FOV will require longer loop cycles to find the beacon [39]. Both Charge-Coupled Device (CCD) and CMOS sensors have typically been used for beacon detection; however, position-sensitive detectors such as quadrant PIN photodiodes and quadrant Avalanche Photodiodes (APD) have also been used for beacon detection [32], [39]. A dominant challenge associated with array-like detectors, however, is the loss of the beam spot if it falls within the dead zone (the space between individual sensors), provided the dead zone is larger than the beam spot width. Additionally, they are subject to crosstalk between individual sensors, which degrades performance [39].

8) MINITURISATION

Miniaturisation of ATP systems is particularly pertinent for receivers onboard LEO nanosatellites where there is a limited budget on Size, Weight, Power, and Cost (SWaP-C). Additionally, nanosatellite platforms thrive on standardised components that interface with standardised satellite busses and other components, as it enables wide compatibility and mass production to reduce costs. The challenge is to maintain (or improve) performance while creating compact components with standardised interfaces. Industry efforts for modularisation and miniaturisation have been realised by the ROKS mission, which has worked closely with commercial partners to design the modules of the mission as individual components that will be sold and integrated into other nanosatellites [34].

9) SATELLITE FLIGHT TIME

The total effective communication time, defined as time during which secret keys can be distributed, is dependent on the satellites total time in pass (i.e. satellite is visible from the OGS), the maximum elevation of the satellite during the pass, and the pointing errors that can cause signal loss. This is mostly a concern for LEO satellites, as discussed in Section I-E. At lower elevations (<20 degrees) channel losses due to the atmosphere can be large enough that communication is effectively impossible, which significantly reduces the total effective communication time. The time for signal acquisition by an ATP system, and pointing and tracking errors after signal lock, can further reduce the total effective communication time.

III. RECEIVER

This section covers telescope systems ranging from large observatory installations to transportable OGSs.

A. ADVANCES IN RECEIVER SYSTEMS

The **QUESS mission** used three separate OGSs to perform entanglement distribution in the downlink channel. The receiving telescopes of the Delingha and Nanshan OGSs have diameters of 1200 mm, while the Lijang station diameter is 1800 mm [5]. After the main telescopes, driven by the ATP system, the quantum signal is separated from the beacon and synchronisation lasers by dichroic mirrors and directed into the analysis module of the receiver. Due to the relative motion of the satellite to the ground, a drift in arrival time and the polarisation observed by the receivers is introduced. To correct for this, two motorised QWPs, a motorised Half-Wave Plate (HWP), a Pockels cell and a 20 nm bandwidth interference filter (to reduce background noise) are aligned in the optical path before the PBS [5]. The polarisation rotation angle offset, and phase shift are tracked and dynamically compensated with the apparatus, resulting in recovering the polarisation contrast to 80:1 [5]. The PBS then measures the entangled photons, forcing them to be detected in either the horizontal or vertical single photon detector. An 850 nm 100 kHz pulsed synchronisation laser is co-aligned and transmitted with the 810 nm entangled photons to synchronise timing at the two OGSs. With a synchronisation jitter of 0.77 ns, the received signals are time-tagged and coincidence detection was performed with a 2.5 ns window [5].

The **QEYSSat payload**, as a generalised receiver, is capable of supporting various polarisation-encoded quantum sources and was tested with BB84 decoy states. In its field trial, it used a 10 cm aperture refractive telescope (Tele Vue

NP101) to collect the signal, which was attached to their FPU, that houses a FSM closed control loop system [32]. The FPU has a FOV of ± 0.3°and the quantum signal is guided through a 50 μm pinhole followed by two 785 nm spectral filters [32]. This connects to the Integrated Optical Assembly (IOA), a passive-basis choice polarisation analysis module, that consists of a traditional BB84 setup: a 50-50 beam splitter and two PBSs [32]. The four outputs of the PBSs are connected to one single photon detector each [32].

The **Zvenigorod Observatory, OGS** is specifically designed for polarisation-encoded QKD. The main telescope is a 0.6 m aperture Ritchey-Chretien design on an Alt-Az mount, with the receiver box mounted on the back of the main mirror [30]. The receiver box consists of the polarisation analysis module and the ATP module. Within the ATP module, after the signal and beacon light are directed to the dichroic mirror by the FSM, the two are separated. The quantum signal is reflected from the dichroic mirror to a beam expander, which directs the signal to a motorised HWP. After which, the signal passes through two 850 nm interference filters before entering the Polarisation Analysis (PA) module. The PA module is a BB84 passive basis choice polarisation analyser and features a 50-50 beam-splitter and two PBS. The four outputs of the two PBSs are connected to couplers that link the signal via optical fibre to a 5-channel single photon detector. The 5th channel is used for synchronisation using the incoming beacon laser.

The **ROKS mission** satellite uses a Schmidt-Cassegrain reflecting telescope, which it calls GARNET, a compact telescope that occupies only 1.5 U of the 6 U nanosatellite platform. It has a 90 mm aperture with 30 × magnification and a FOV of ±0.25°; which is the largest size aperture that can be accommodated in a 6U platform without resorting to deployable optic solutions [34]. The Schmidt plate of the telescope design allows for a compact telescope with fast optics and offers a wide FOV by correcting for aberrations. GARNET interfaces with the ATP system directly, and all incoming or outgoing signals are directed through the telescope and kept in alignment by a MEMS mirror. ROKS also uses a modified forward-looking imager, FLI-NT, to detect cloud coverage during night operations. FLI-NT is designed to look ahead of the satellite's flight path and determine cloud conditions, advising the Onboard Computer (OBC) whether communications with an OGS will be cloud-obstructed. The OBC is then programmed to adapt the satellite scheduler, opting to continue generating random numbers in preparation for downlink transmission or to begin the QKD protocol with the OGS [34].

The **Mount Stromlo OGS** is equipped with an AO system comprised of 277 actuators and is a main focus of the OGS [33]. The main receiver telescope is a R700 0.7 m aperture Ritchey-Chretien design from PlaneWave Instruments. After coarse pointing is established, the signal is received by the main telescope and is connected via the telescope's Coudé path to the FSM, which corrects lower order residual jitter and guides the signal to the AO system, which then provides higher order corrections [33]. The FSM and AO system have a Shack-Hartmann wavefront sensor [33], as part of a closed control loop. The Mount Stromlo OGS, as a generalised receiver, does not have any specific protocol optics; however, by directing a signal via the Coudé path to one of four labs beneath the dome, it can accommodate any additional receiver optics for any QKD protocol.

A summary of the advances and suggested improvements for LEO nanosatellite QKD mission receivers is given in Table 2.

B. RECEIVER SYSTEMS CHALLENGES AND LIMITATIONS

The overall receiver system of a LEO nanosatellite QKD is primarily concerned with minimising optical signal losses within its components and those induced from atmospheric effects (as discussed in Section I-C). Several challenges facing receiver systems, as well as intrinsic limitations, are presented in this section. However, given the overall complexity of the LEO nanosatellite QKD environment, it should not be considered exhaustive. Additional challenges are often attributed to LEO nanosatellite receivers, due to limited resources of volume, mass and power. A theoretical model of a receiver system that expands the basic system by including the advances seen in the missions studied is shown in Fig. 3.

1) TELESCOPE APERTURE SIZE

The aperture size of the telescope can be a limitation for receivers. The aperture size of the receiving telescope is positively correlated with the gain. Aperture size is often limited by volume for nanosatellite platforms and limited by manufacturing and maintenance costs for optical ground stations. The QUESS quantum entanglement distribution mission used two OGSs with aperture sizes of 1.2 m and 1.8 m in diameter [5], while the Mount Stromlo OGS uses a 0.7 m aperture telescope [33] and the Zvenigorod Observatory uses a 0.6 m aperture telescope [30]. For LEO satellite-based receivers, the QUESS quantum teleportation mission used a 0.3 m telescope [42] while the QEYSSat mission, in its field-testing, used a 10 cm aperture telescope for its receiver [32]. LEO nanosatellite QKD system designers should typically aim for a minimum aperture size for the receiver (either onboard the nanosatellite or on the ground) that will meet the requirements, calculated from the link budget for the system, and under the constraints of volume and cost that may be applicable. Nanosatellite platforms are unlikely to support aperture sizes larger than about 10 cm while still adhering to a bus size of 1-6 U, presenting a severe limitation to the achievable receiver gain in LEO nanosatellite QKD missions with a satellite receiver.

2) BACKGROUND LIGHT AND DAYTIME OPERATIONS

As discussed previously in Section II-C for two-way beacons, background light also presents a major challenge to the quantum signal receiver system. The primary sources of

TABLE 2. Advances in receiver systems and suggested improvements.

Advances in receiver systems	Suggested improvements to receiver systems
Miniaturisation of space systems from small-sat to nanosatellite platforms [34].	Photonic Integrated Circuits (PIC) for receiver optics, dichroic mirrors, beam-splitters, and polarisation rotators.
Mobile OGSs are being developed, allowing for flexible station locations instead of fixed observatories [40].	Optical fibre for connecting PIC components.
Satellite telescopes have utilised Schmidt-Cassegrain designs for compactness and wider, useful field of view [34].	Improvements to coupling techniques and optical adhesives to reduce coupling losses.
Forward-Looking Imaging Camera has been used for cloud detection, enabling autonomous satellite scheduling [34].	
Adaptive optics is planned for use on large observatories for quantum communication [33].	
MEMS mirrors have been used instead of fast steering mirrors [34], [41].	
Liquid crystal polarisation rotators have been used instead of motorised wave plates to reduce micro-vibrations on satellites [38].	

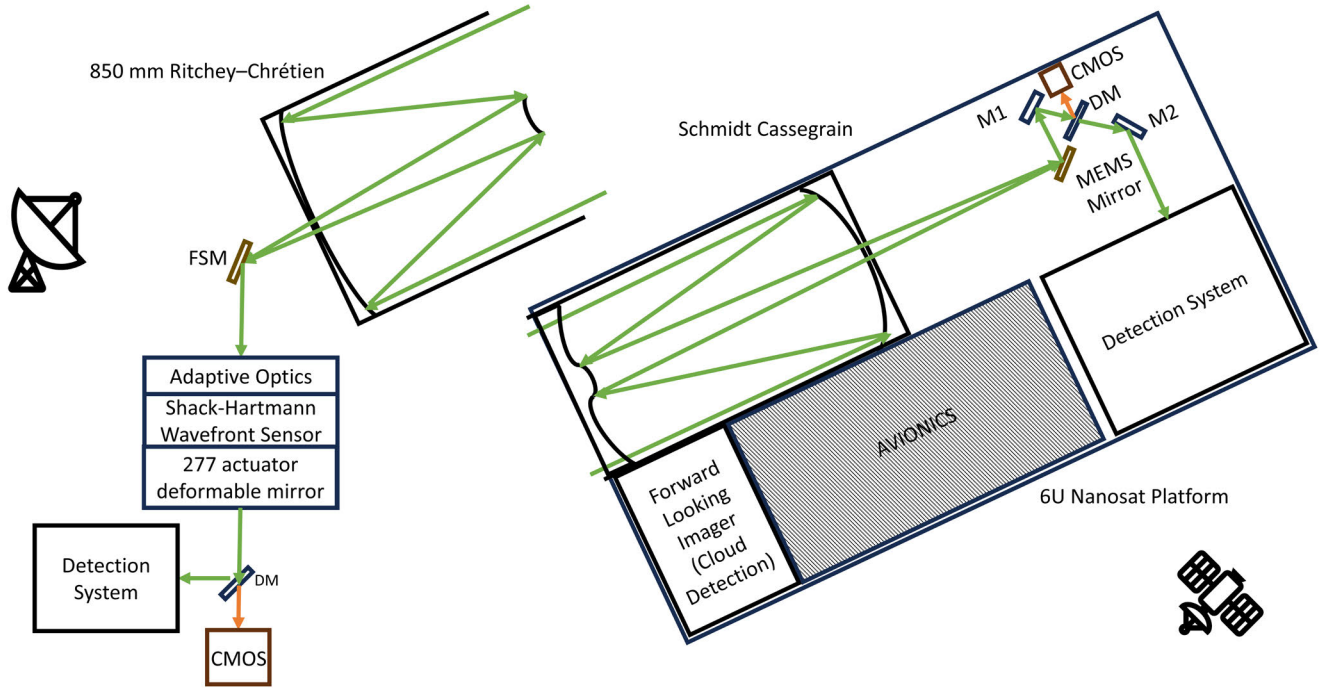

FIGURE 3. Advances in receiver systems for OGSs and satellites. The quantum signal is denoted by green. Beacon Rx, in the receiver's frame of reference, is denoted by red. Beacon TX is omitted for clarity.

background light in a LEO nanosatellite QKD mission are the Moon at night and the Sun during the day. For receivers onboard nanosatellites, additional sources of background light will arise from the surface albedo of Earth within the telescope's field of view. Both the QUESS and QEYSSat field tests only performed experiments at night [5], [32], with performance expected to degrade to unfeasible if a link is attempted during the day due to the much greater source of background light emitted by the Sun. The quantum signal can be considered to be much more susceptible to background light than the two-way beacon lasers due to its inherently weak optical power. In rural settings, commercially available spectral filters with a bandwidth of 1 nm can restrict background light, but they are less effective in an urban environment [41]. Spectral filters with a bandwidth of 0.05 nm can permit daytime operations; however, with narrower filters, the Doppler shift of a LEO satellite needs to be accounted for during the pass, requiring active tuning of the spectral filter to within 0.02 nm [41]. Alternatively, if a coherent detection system is used for the QKD protocol, background light will be less of a challenge or limitation, as the local oscillator effectively acts as a matched filter. This removes the requirement for extra temporal, spatial and/or spectral filters. Overcoming background light will result in a stronger link for the quantum link, thus fewer errors and a more secure connection, and a larger transfer rate for data, as links will not be restricted to only moonless nights.

3) QUANTUM SIGNAL WAVELENGTH

The wavelength of the quantum signal may be driven more by the quantum source, but consideration for the receiver and detection system is also necessary. The primary factors that influence the quantum signal wavelength selection are similar to those that affect the beacon wavelength choice in ATP systems, as discussed in Section II-C. Additionally, however, the wavelength choice for quantum signals must also consider: the potential wavelengths able to be generated by a quantum source, and the wavelengths of classical signals or beacon signals and how they are multiplexed with the quantum signal. Studies on wavelength selection for quantum signals have been performed in literature [43]. The quantum signal wavelength will dictate the materials and design of the receiver and detection system, necessitating trade-offs.

4) OPTICS DEGRADATION

Optics degradation due to the environment of space is a challenge for LEO nanosatellite QKD receivers. It is caused by atomic oxygen, thermal stress, electromagnetic radiation, telescope outgassing, charged particles, space debris and micro-meteorites; and the dominant source of degradation in LEO is atomic oxygen, which corrupts mirrors and can react with organic materials to produce a volatile compound that condenses on mirrors [44]. Primary optics for telescopes are typically mirrors instead of lenses due to several factors, including: being operational over a wider spectral range, easier to manufacture in different shapes and sizes, and their suitability for scanning devices [44]. Mirrors consist of a substrate and a coating, and substrates are chosen based on specific stiffness, thermal stability, space environmental resistance, achievable surface quality, weight, and cost. The most common coatings for space grade optics operating in the Ultraviolet (UV) to Infrared (IR) range are Ag, Al, Au, or Be, due to their reflectance at wavelengths of interest (e.g. a wavelength for a quantum signal) [44]. Reflectance vs wavelength plots for several of these common coatings can be seen in Figure 4. The choice of coating is also dependent on durability and cost. A material may have good reflectance for a wavelength of interest, but require additional protective coatings for the space environment that reduce the overall reflectance of the mirror. In general, Au can achieve a reflectance of around >96% for wavelengths between 700 nm and 2000 nm, Ag can achieve a reflectance of around >98% for wavelengths between 500 nm and 800 nm, and Al can achieve a reflectance of around >96% for wavelengths between 1500 nm and 2000 nm. Silver coatings tend to tarnish, which limits the lifetime of the mirror, but they have a higher damage threshold than aluminium mirror coatings.

To ensure suitability for an LEO environment, optical components undergo exposure to 5 eV energy atomic oxygen during space qualification, where the atomic oxygen fluence and exposure time are adjusted for the mission lifetime [44]. The most common strategy for reducing atomic oxygen erosion of materials in space is the application of thin-film protective coatings composed of dielectric materials [44]. Careful selection of substrate materials and coatings remains the conventional approach to mitigate the degradation effects of space, except for micro-meteorites. Micro-meteorites can blast away the coating, exposing the substrate, crack the mirror, or even result in the destruction of the satellite. The current mitigation strategy against micro-meteorites and space debris depends on prevention by reducing space debris and prediction by tracking it [44].

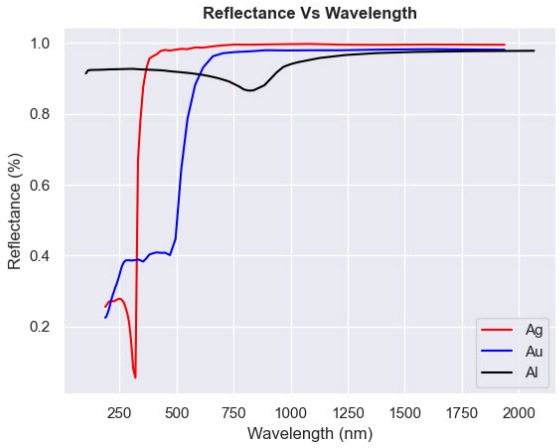

FIGURE 4. Reflectance vs wavelength for several of the most common coatings for space grade optics. Optical constants data were taken from previous studies [45], [46]. Differences in reflectivity in other studies can often be attributed to differences in the composition and thickness of protective coatings [44].

5) MINITURISATION

LEO nanosatellite QKD receivers are severely limited in volume, mass, and power, which presents a considerable challenge. Miniaturisation of common QKD systems will provide a solution, but achieving it remains a challenge itself. Photonic Integrated Circuits (PICs) designed explicitly for QKD applications have been built, albeit for quantum source transmitters. The QUICK^3 mission uses a PIC to build a Mach-Zehnder interferometer with a volume of $45 \times 24 \times 1$ mm^3; fabricated by Femtosecond Laser Micromachining (FLM) [47]. Other optical components that have been built using FLM include beam splitters, polarisation rotators, fibre Bragg gratings, and waveguides in any desired direction, leading to very compact photonic designs with high performance [47]. These same techniques could feasibly be applied to LEO nanosatellite QKD receiver and detection systems, enabling high performance within the small form factor of a nanosatellite.

6) SITE LOCATION

The site location for optical ground stations can have a significant impact on the overall receiver and detection system performance. Several considerations include: local climate and weather patterns (average cloud coverage, average precipitation, average wind speed, atmospheric

chemical composition, etc), visibility conditions (obstruction to view, trees, buildings, mountains, etc), access to existing infrastructure (power, consumables like coolant, staffing, telecommunications, internet, etc), local electrical noise, light pollution, and seismic activity. Laser safety is another aspect that must be considered, which requires careful evaluation of the impact on flight traffic when in proximity to airports.

Typical astronomical sites may be an attractive option for an OGS site due to clear skies and less light pollution, but the presence of a two-way beacon system and the quantum signal will introduce light pollution to astronomical applications, making it unfeasible to share the space. Additionally, these locations are typically rural, while end users of quantum communications will generally be located in cities, and due to the weak quantum signal, its inability to be amplified, and high losses in optical fibre channels, there is more value for OGS to be located near cities for LEO nanosatllite quantum communications. The trade-off here is the increased background light from light pollution.

The Earth's atmosphere is highly turbulent and causes significant variations to optical beam propagation, both spatially and temporally, due to random variations in temperature and pressure. This can be pre-compensated for using adaptive optics techniques as previously described in Section II-A and theoretically studied for uplinks to LEO and GEO satellites [48]. The effect of adverse weather conditions such as rain and atmospheric turbulence has been studied in [43] for two scenarios: (i) a clear summer's day in Tucson, Arizona (an ideal location for satellite communication), and (ii) an overcast winter's day in Ireland. MODTRAN (Moderate resolution atmospheric transmission) toolkit was used to model atmospheric propagation of light in the 200 nm −100 mu m spectral range [49], [50], providing atmospheric extinction (due to aerosol absorption and Rayleigh/Mie scattering) and spectral radiance. As expected with the AO system combined with spatial, spectral and temporal filtering, the secret key rate is higher in Tucson, but on a relatively clear winter's day in Waterford, it is possible to yield high secret key rates due to low solar radiance.

Additionally, cloud coverage and its ability to block signal transmission, is a significant limitations to LEO nanosatellite QKD systems. Current strategies centre around OGS site diversification to increase potential satellite coverage by either installing multiple OGS at weather diverse locations or through portable OGSs that are deployed to sites when and where they are required. Several portable OGSs have been developed for classical optical communications, including a transportable OGS designed by DLR, a 600 mm aperture Ritchey–Chrétien telescope with 1550 nm beacon lasers and a mass of around 500 kg [51]. Smaller designs for classical optical communication include a portable 355 mm aperture OGS by Astrolight Space, and TERRA-M, a 300 mm aperture portable optical ground terminal by Archangel Lightworks [40]. Converting the use case to quantum communications may present a small challenge, but considering the overlap in hardware between the two systems, it should not be insurmountable, and is promising.

For site diversification through multiple OGS, a study by the QUARC mission was undertaken where 43 sites for OGSs within the United Kingdom were identified, and the generated secret key rate for QKD was simulated using historical weather and seasonal data and a 700 mm aperture receiving telescope from a 90 mm aperture LEO nanosatellite transmitter [41]. It was found that weather and cloud coverage, along with suitability for QKD, assuming only night operations, vary with the season and length of day, with some sites more attractive than others at different stages of the year. Site surveys are a vital component to site diversification, either for identifying sites for multiple OGSs or for locations for a portable OGS, and will remain a key component to overcoming the challenge of cloud coverage to quantum communication receivers and detection systems.

7) BEAM SPOT SIZE AND ELEVATION ANGLE

As a Gaussian laser beam propagates, diffraction causes its beam profile to spread depending on its wavelength, initial spot size, and propagation distance. The free-space (geometric) coupling efficiency at the receiver depends on the diameter of the receiver aperture and the beam waist at the receiver. The increased beam spot size at the receiver due to diffraction is responsible for significant power loss in the satellite downlink scenario. Increasing the initial beam waist or the receiver diameter will increase the geometric coupling efficiency, whereas decreasing the wavelength or propagation distance decreases the coupling efficiency. Careful consideration should be given to this multiparameter space during the design phase of the optical ground station in order to optimise the performance of the receiver by maximising detection efficiency [43].

A theoretical analysis of the effect of the Earth's atmosphere on the performance of a LEO satellite-to-Earth quantum communication channel as a function of the ground observer's zenith angle, geographical position, and orbital inclination of the satellite has been previously presented in literature [52]. The transmitter laser beam was shown to distort due to atmospheric refraction, absorption, and turbulence at large zenith angles and when the satellite is close to the horizon. This is due to the reduced transmittance of light for large slant angles where the beam has a larger propagation length through the atmosphere (which is strongest close to the Earth's surface).

IV. DETECTION SYSTEM

Detection systems vary depending on the QKD protocol selected and can be divided into two categories: Single Photon Detectors (SPD) or coherent detectors. This section discusses the advances in the two detection system types separately. The majority of practical implementations of satellite quantum communications have used the polarisation-encoded decoy state BB84 QKD protocol with SPD receivers. This is due in part to the maturity of the

protocol, both in implementation and security proofs, and to the phase changes from atmospheric effects that make CV-QKD extremely difficult.

A. ADVANCES IN DETECTION SYSTEMS

The latest developments and research of several detection system technologies are discussed in this section.

1) SINGLE PHOTON DETECTORS

Photomultiplier Tubes (PMTs) are an easily available SPD and have demonstrated QKD with Corner Cube Reflectors (CCRs) for signal wavelengths around 800 nm using two Hamamatsu H7360-02 PMTs with a detection efficiency of around 10% [53]. This is quite poor for satellite quantum communications and is not recommended.

Silicon Single Photon Avalanche Diodes (Si-SPADs) are currently the most popular SPD for detection systems on LEO quantum communications nanosatellite missions. They are used on the QUESS satellite, Micius [42], QEYSSat satellite receiver [32], and the Zvenigorod OGS [30]. Their popularity stems from being one of the more mature single-photon detector technologies, having been ubiquitous in applications ranging from light detection and ranging, laser time transfer, deep-space communications and quantum communications for the last two decades [54]. Significant work was done during the QUESS mission to adapt COTS Si-SPADs to a space environment, with emphasis on low noise and high reliability [54]. Following the trend towards nanosatellites, passively quenched Si-SPADs have been flown successfully on two nanosatellite missions, Galassia [36], a 2U platform and SpooQy-1 [38], a 3U platform, demonstrating their small volume suitable for nanosatellites and flight heritage. At optical wavelengths, they have a quantum efficiency of around 50% at 900 nm and 65% at 830 nm, based on the SAP500 model by Laser Components as used in the SpooQy-1 mission and the QUICK^3 mission to test a novel single photon source [47]. For QEYSsat, using the Excelitas Technologies SLiK Si-APD, they achieved a detector efficiency of around 45% with passive quenching and thermoelectric cooling to -20°C [32] while the Zvenigorod OGS used Si-SPADs with a quantum efficiency of 50% at 850 nm [30]. QUESS also opted for Excelitas SLiK Si-SPADs, achieving efficiencies greater than 45% at 780 nm after 1029 days in orbit [54].

SpeQtral Pte. Ltd. uses three SAP500 model Si-SPADs on a nanosatellite platform for its detection system [47]. Dark counts are a concern and are dependent on temperature. Cooling is often a solution, but for a nanosatellite, an active cooling system will put pressure on the limited available power. Thermoelectric coolers (TEC) for nanosatellites have been developed as a solution [47]. Jitter time can be lessened by integrating an active quenching circuit, which assists in lowering and restoring the bias voltage with additional electronics to increase the recovery time and create a well-defined dead time. The dead time of the detection system used by SpeQtral Pte. Ltd. was reduced from greater than 1 μs to 60 ns using an active quenching system [47].

SNSPDs can offer better system detection efficiencies than Si-SPADs, at around 80% at 850 nm [55] or 98% at 1550 nm [56]. SNSPDs have even been built to have relatively high System Detection Efficiencies (SDE) (30% at 800 nm, 73% at 1271 nm, and 60% at 1550 nm) over a broad spectral range from 532 nm to 1640 nm [57]. Recent work shows that unity internal detection efficiency at wavelengths in the mid-infrared has been achieved, from 10 μm up to 29 μm, with possible extension to even longer wavelengths [58]. Other recent work has shown that SNSPDs are also capable of photon number resolution (PNR), detecting individual photons that may have hit the detector simultaneously, resolving up to seven photons [59].

SNSPDs are the dominant technology for state-of-the-art research in fields which rely on single photon detectors, and this is true for LEO nanosatellite quantum communications when these devices can be accommodated. SNSPDs offer extremely high detection efficiencies (often near or at unity), very low dark count rates, low timing jitter and picosecond time resolution [56], [60]. The performance of SNSPDs has been improved over two decades with several breakthrough techniques that have improved the detection efficiency. These include: meandering nanowires to increase the active area, improving coupling between the SNSPDs and the carrier medium with optical nano-antennae structures, integrating optical cavities with the SNSPDs, combining two SNSPDs in parallel, improving coupling further with photonic waveguides and using different material stacks (NbN, MoSi, NbTiN instead of WSi) [60].

The SNSPD principle of operation necessitates cooling to below the superconducting critical temperature of the SNSPD, which is around 10 K for a typical NbN superconducting film or 15.51 K for an NbN film on an AlN/Si substrate annealed at the optimum temperature for the substrate element composition to increase the grain size and crystallinity of the film [61]. The detection efficiency of SNSPDs also depends significantly on temperature; the detection efficiency will drop when operated at higher temperatures, which also increases the dark count rate and time jitter, further reducing the overall SNR of the system [60]. Increasing the superconducting critical temperature of SNSPDs is an active and challenging area of research, but recent work has demonstrated single photon detection up to temperatures of 25 K [62].

Superconducting Microstrip Single Photon Detectors (SMSPDs) are a recent development on SNSPDs and have wider micrometre lines instead of 40–120 nm nanowires. They have larger critical currents and lower kinetic inductance, which enables them to have much larger active areas [60]. SMSPDS, with an active area of 50 μm diameter, have demonstrated an SDE of 92.2% at 1550 nm, with a dark count rate of 200 cps, a time jitter of 48 ps at 0.84 K or an SDE of over 70% at 1550 nm at 2.1 K [63]. This was achieved using Electron Beam Lithography (EBL) and the NbN film

was He ion irradiated, which is known to improve the Intrinsic Detection Efficiency (IDE) of the microstrips [63].

Other works have demonstrated that SMSPDs can be fabricated using UV photolithography (instead of EBL) since the requirement on the width precision of the strip is lower than that of SNSPDs, which reduces the time cost and process flow of SMSPD fabrication [64]. The SMSPD produced using UV photolithography, with an active area of 1000 × 1000 μm, was shown to have an SDE of 7% at 1550 nm with a time jitter of 144 ps and near unity IDE up to 800 nm; the low SDE was attributed in part due to not using He ion irradiation, and it is expected that applying this technique along with other improvements will increase this substantially [64].

SMSPDs can provide a high timing performance and high detection efficiencies for a much larger active area than current SNSPDs using single-mode fibre coupling. Recent work has demonstrated free space coupling with a large active area SMSPD of around 260 μm, obtaining an SDE of 2% for 1550 nm at 2 K and a DCR of 5 kcps with time jitter of 171 ps; although the low SDE is expected to improve with future enhancements such as lowering the operating temperature to 0.85 K, adding new geometric designs and integrating with an optical cavity [65]. Free space coupling to SNSPDs or SMSPDs currently results in significantly lower detection efficiencies than single-mode fibre coupling, but continued work in this area could lead to similar SDEs.

Increasing the active area of a SNSPD detection system can also be achieved with arrays of SNSPDs, and is an active, challenging area of research [60], [66], [67]. SNSPD arrays with active areas of 1.6 × 1.6 mm have demonstrated an SDE of 8% at 1550 nm with comparable time jitter and lower dark count rates than SPADs, despite having much worse detection efficiency and uniformity [67]. This is promising, however, as it is expected that with enhancements to the design, the efficiency of an array of SNSPDs can be improved to similar levels to what they exhibit individually, benefiting from larger active areas. The disadvantages of SNSPD array detection systems are an increase in fabrication and readout complexity, along with low output pulse amplitudes. This has necessitated specialised equipment and cryogenic engineering to overcome the accumulated heat load from high-speed cables (with direct detection for each SNSPD) [66], [67]. Recent research has been focused on improving the scalability of the readout mechanism to allow larger and more efficient arrays of SNSPDs [66].

Coupling can represent a significant loss in system detection efficiency for all single photon detectors, but recent work with PICs may offer solutions. Lithium Niobate On Insulator (LNOI) is considered a better material than silicon due to its large transparency window, strong second-order nonlinearity, the possibility for periodic poling and access to fast and low-loss switching using the electro-optic effect [68]. SNSPDs have been integrated onto on-chip optical waveguides in LNOI material platforms, and even with electro-optic switches integrated on the same chip and operated at cryogenic temperatures with some success; although, semiconductor detectors, like SPADs, have also been integrated on LNOI platforms, but with less success [68].

The high efficiencies of SNSPDs are attractive for LEO nanosatellite quantum communications, but their requirements of cryogenic cooling and coupling to fibre optic cable make them unwieldy and prohibitive. Within an OGS, an environment for SNSPDs can be accommodated, but it is currently infeasible to use them as part of a nanosatellite receiver and detection system. The ongoing research to reduce the strict temperature requirements and increase the active area of SNSPDS or SMSPDs is promising and may enable smaller form factors for these detection systems by removing the need for cryogenic cooling and enabling easier coupling for free-space optical signals.

One promising solution for overcoming the time resolution of a detector is to increase the number of QKD channels by demultiplexing emitted polarisation encoded entangled photons according to their frequency correlations, reducing probability of reaching the limits imposed by the time resolution of individual detectors, and opening up the possibility of using an ultra-bright pump source [69]. The concept was implemented by two-photon frequency-polarisation hyper-entangled states with a ppKTP crystal in a Sagnac configuration, which generated collinear degenerated type-0 SPDC and then entangled the two emitted photons in polarisation [69]. The two photons were then guided to the demultiplexer, where Volume Bragg Gratings (VBGs) were used to separate the photons by frequency. VBGs and Si-SPADs were used to demonstrate the usefulness of mature space-ready components, but using more novel detectors, with finer time resolution, could increase performance further by lowering the required coincidence period for a detection. Additionally, one could take advantage of new developments in PICs and use fibre Bragg gratings etched in waveguides instead of VBGs [47].

2) COHERENT DETECTORS

Homodyne and heterodyne detectors are required for CV-QKD, and they aim to measure the in-phase and quadrature signals of a received state in phase space as accurately as possible. The steps that this section outlines for CV-QKD systems follow a current state-of-the-art review [3], and for a more comprehensive review on the state of the art for all CV-QKD systems, not only satellite quantum communications systems, the reader is directed towards it. Typically, a receiver has several components to its configuration, including monitoring, demodulation, detection, Shot Noise Unit (SNU) calibration and signal processing.

CV-QKD requires having a carrier signal, produced by a local oscillator, alongside the modulated quantum signal. Historically, CV-QKD systems have used Transmitted Local Oscillators (TLO) (or in-line LO), which multiplex the quantum signal with the LO via Time Division Multiplexing (TDM) using pulsed laser light to reduce crosstalk, at the

expense of a requirement for a high extinction ratio to isolate the signals. Systems that do not transmit the LO but instead generate the LO at the receiver, so-called Local Local Oscillators (LLO), reduce the requirement for isolation between the quantum and classical signals as the pilot tone which will be used to monitor phase recovery is not required to be as high in power as a transmitted LO, so it can be multiplexed either by TDM or Wavelength Division Multiplexing (WDM) without a high requirement of isolation. The demand for increasing data rates, and that it becomes harder to achieve a sufficient extinction ratio between the quantum signal and the classical signals at higher repetition rates, has led to continuous wave CV-QKD with a pilot tone multiplexed by WDM using an LLO becoming popular in recent years [3].

The CV-QKD receiver chain has been described previously in literature [3]. In summary, the receiver chain is comprised of several stages:

1) **Monitoring.** The monitor tracks the wavelength, frequency, power, and amplitude of the LO (for TLO schemes) or the pilot tone (for LLO schemes), and is vital to TLO schemes due to the potential manipulation of the LO by a third-party eavesdropper. Monitoring is also an effective safeguard against any injected light attacks which could be deployed to attempt to disrupt detection or the SNU calibration process.
2) **Demodulation.** This stage compensates for effects that disrupt polarisation and phase of transmitted signals, and for pulsed CV-QKD systems, the demultiplexing of the quantum and classical signals. This includes both fast (due to channel disturbances, like those generated by atmospheric effects) and slow (due to an optical path difference) fading types of phase mismatch. Additionally, the frequency drift between the incoming quantum signal laser and the LO laser in LLO systems is also typically compensated. Clock synchronisation is a vital part of the stage that aligns the sampling points at the transmitter with those at the receiver. Continuous-wave CV-QKD systems tend to approach demultiplexing, polarisation/phase compensation and clock synchronisation in the digital domain after detection through DSP.
3) **Detection.** Homodyne detection is the primary method of measuring quantum signals in a CV-QKD system. In homodyne detection, the quantum signal and LO are interfered with by a 50:50 coupler and the two interfered output signals are detected by two photodiodes. The resulting photocurrents are then combined into a differential current, which holds the information on one of the quadratures of the quantum signal. As the homodyne detector only measures one quadrature at a time, and security analyses require both quadratures to be detected, a phase modulator is used on the incoming LO before the coupler to randomly switch between in-phase (0) and quadrature ($\frac{\pi}{2}$) components and thus satisfy the collection of statistical data for both quadratures. Of course, this leads to the immediate benefit of a heterodyne receiver: adding another homodyne receiver such that each receiver is dedicated to monitoring either in-phase or quadrature data by using a permanent phase difference of ($\frac{\pi}{2}$) for one arm of the split LO, ensures that both quadratures can be detected and saved simultaneously.
4) **Shot noise unit calibration.** The SNU is the variance of the shot noise, with the variance of the quantum fluctuations on the phase space of vacuum states defined as unity. It is vital to establish the background variance of the shot noise through measuring a statistically significant number of vacuum states, so that the variance of the incoming signal states can be compared against it, and the security of the channel can be determined.
5) **Digital signal processing.** DSP is used to replace several analogue components in the typical receiver chain for coherent detectors, both classical and quantum. With some exceptions, DSP algorithms can be used in both systems (as discussed in Section I-D). DSP algorithms have been used in quantum communications to perform: demultiplexing, clock synchronisation, static equalisation, S21 compensation and removing the signal pulse, downsampling, dynamic equalisation, and frame synchronisation [3]. DSP parameters are typically adjusted dynamically with the system to optimise performance, and as such are an excellent candidate for machine learning applications, which have already been applied to phase estimation with good results [3]. After DSP is completed, the data is then sent to the post-processing stage.

For LEO satellite CV-QKD communications, a Delay-line LLO (D-LLO) scheme has been proposed using TDM for a pulsed quantum signal and pilot tone [70]. In the receiver, self-coherent LO pulses are sent to two heterodyne detectors. The transmitted reference and modulated signal pass through adaptive optics and are separated by a polarising beam splitter. The reference pulse is sent to one heterodyne detector, the result of which is used to correct both the reference and modulated signal for phase changes occurring due to transmission. The modulated signal is sent to the other heterodyne detector for demodulation. Figure 5 gives the schematic of the D-LLO protocol as described in the literature.

Implementations of CV-QKD systems in nanosatellite LEO communications are extremely scarce; however, demonstrations of GEO small-sat CV-QKD feasibility have been successful at preserving quantum coherence [71]. To achieve this, a continuous-wave, Gaussian-modulated BPSK coherent state, LLO, homodyne detection configuration, with an AO system to correct for wavefront disturbances and to launch the incoming signal into a single-mode fibre, was used cite RN200. By mode matching the LO to the incoming quantum

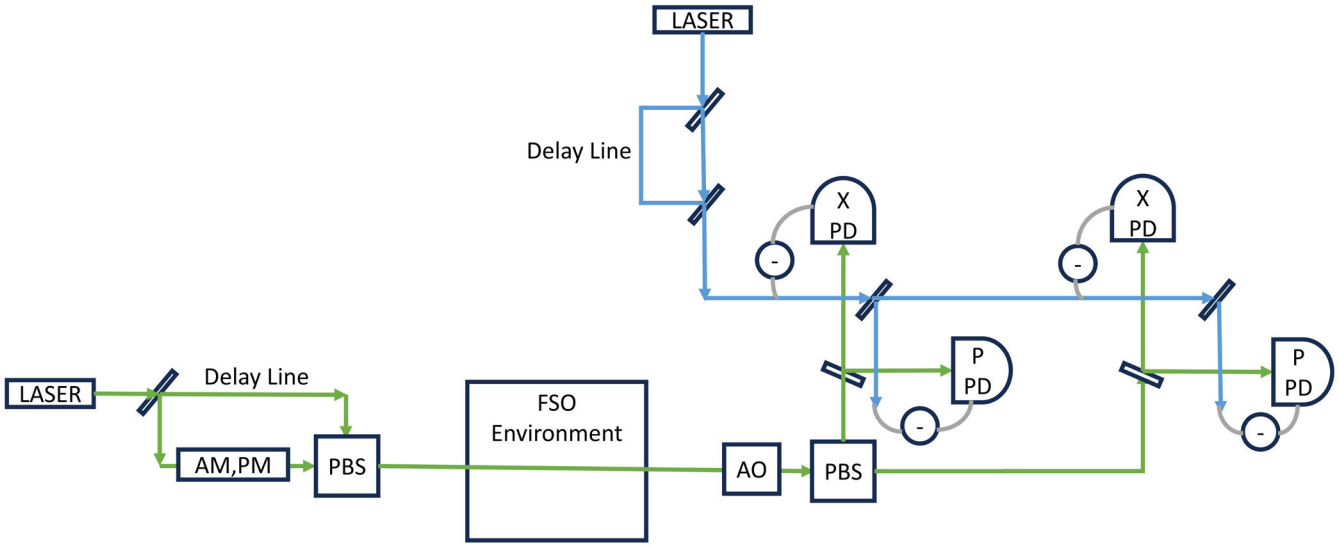

FIGURE 5. Schematic of the D-LLO protocol. The quantum signal is denoted by green, and the LLO signal is denoted by light blue. AM: amplitude modulation. PM: phase modulation. PBS: polarising beam splitter. AO: adaptive optics. PD: photodetector.

signal, any stray light was filtered out, showing that daytime operations did not create operational constraints.

B. DETECTION SYSTEMS CHALLENGES AND LIMITATIONS

Challenges and limitations associated with detectors will differ between ground-based detection systems in OGSs and nanosatellite detection systems, typically due to the natural design constraints related to nanosatellites (SWaP-C). This section discusses several challenges and limitations of both single-photon detection and homodyne detectors. For brevity, the discussion is restricted to the detection efficiency of single-photon detection systems and several factors impacting homodyne detectors.

For all QKD protocols, there exists an error rate threshold that represents the maximum error rate the link can sustain while ensuring secure communications by verifying that a third-party eavesdropper is not present in the link. For CV-QKD, errors are typically measured in the excess noise of the system and for DV-QKD, they are measured by the quantum bit error rate.

The quantum state's high volatility and susceptibility to decoherence require additional techniques within the receiver detection system to handle these losses. In addition to AO systems, several theories and simulations use temporal and spectral filtering to reduce losses in free space and satellite QKD [4], [11], [72]. Many satellite-to-ground channel models estimate losses, such as the Micius satellite, where the minimum total system loss at zenith angle was calculated to be 34 dB. This consists of diffraction-induced beam broadening during propagation, pointing jitter, atmospheric attenuation, receiver optical and quantum efficiency loss, and atmospheric extinction loss. Lanning et al. developed a rigorous framework for analysing spatial, spectral and temporal filtering for optimising the performance of free space quantum communication networks [73].

There are several sources of noise at the receiver, and various advances have been made to mitigate the noise effectively during measurements. Spatial filtering at the diffraction limit removes optical noise at the field stop of an optical receiver by limiting the number of sky noise photons that reach the quantum detector. Narrow spectral filtering blocks optical photons outside the bandwidth of the filter. Temporal filtering and the optimal size of the signal window are related to the overall timing jitter of the system due to the detector jitter and electronic response time. Quantitative results from [74] showed that a secure key rate of 191.11 kbps was obtained from a BB84 QKD system lasing at a wavelength of 785 nm under daylight conditions over 275 m with 1 nm spectral bandpass filter, 2.5 ns temporal filter and further filtering to 1.75 ns signal window and a FOV of 283 μrad.

A summary of the advances seen in the reviewed missions and suggested improvements is given in Table 3.

1) SINGLE PHOTON DETECTOR CHALLENGES

The detection efficiency is a crucial concern for both ground and space segment detection systems and is affected by several factors, which differ between various detection system technologies. SPAD efficiencies are influenced by the temperature and the voltage over breakdown at which they are operated (the temperature and overvoltage dramatically affect the dark count rate), and additionally, the jitter time, the time it takes to return to the initial bias. For SPADs on board a nanosatellite platform, the challenge is to optimise for the highest possible detection efficiency while trading against the power consumption needed for overvoltage, cooling, and active quenching, which will be limited. SPADs in

TABLE 3. Advances in detection systems and suggested improvements.

Advances in detection systems	Suggested improvements to detection systems
The miniaturisation of space systems from small-sat to nanosatellite platforms [34], [36], [38].	Implement demultiplexing systems in OGS detection systems.
Photonic integrated circuits (PIC) for some detection system components [47].	Implement demultiplexing systems for nanosatellite systems.
Thermoelectric cooling (TEC) systems on nanosatellite platforms [47].	PIC for detection system optics, dichroic mirrors, beam-splitters, and polarisation rotators.
Si-APD thermal annealing for small-sat systems [32], [54].	Improvements to coupling techniques and optical adhesives to reduce coupling losses.
Radiation shielding for small-sat systems [54].	
Lab demonstrated polarisation entangled demultiplexed Systems [69].	
Fibre Bragg gratings (FBG) are seen on nanosatellite systems [47].	
Femtosecond laser micromachining as a process to fabricate PICs [47].	

ground-based detection systems will still need to optimise these parameters for the optimum detection efficiency, but may not be as limited. SPAD efficiencies are also intrinsically limited by the wavelength choice of the signal (together with the corresponding material composition and design of the semiconductor that will determine its spectral response for a given wavelength).

As discussed in section IV-A1, SNSPDs offer better detection efficiency than SPADs, but the temperature of the system must be reduced to below 10 K, which requires cryogenic cooling. This significantly increases the footprint, cost, and energy consumption of the detection system. For ground-based receivers, this may be acceptable, but it is currently prohibitive for nanosatellite platforms. Onboard a nanosatellite, SNSPD detection systems will be unfeasible until either the superconducting critical temperature can be raised much higher or cryogenic cooling systems can be significantly reduced in volume, mass and power.

An SNSPD detection system for an OGS would significantly boost the detection efficiency of the system; however, the active area of single-pixel SNSPDs is typically around 20 μm, due to trade-offs between the active area, dark counts and the time jitter [60]. This small active area can be challenging for efficient coupling with free space optics, so SNSPDs require fibre coupling with a telescope, which will necessitate an adaptive optics system to be installed. As discussed earlier in section IV-A1, SMSPDs and SNSPD arrays may be able to replace individual SNSPDs and remove the requirement for fibre coupling due to a larger active area; however, much more work is required to improve the detection efficiencies of these technologies to parity with individual SNSPDs.

The environment of space presents additional challenges to detection systems implemented on LEO nanosatellites. All components degrade over time after exposure to extreme thermal cycling, heavy-dose radiation, and micrometeorite impacts. The QUESS team monitored the performance of the Si-SPAD on board the Micius satellite for 1029 days and managed to achieve a dark count increase of only 0.54 cps/day; using a solution of 12 mm thick aluminium and 4 mm thick tantalum radiation shielding, a multistage active cooling system reducing temperature to as low as -60°C, configurable electronics controlling the overvoltage of the Si-SPADs, and thermal annealing [54]. Numerical analysis showed that without these mitigation strategies, single photon detectors with a conventional increase of 30 cps/day would be unusable for quantum communications using decoy-state QKD after 30 days, compared to Micius, which was predicted to last for 4.6 years at an increase of 0.54 cps/day [54]. QEYSSat will use a combination of thermal and laser annealing of the Si-SPADs in the receiver to mitigate dark counts [32]. Micius and QEYSSat are both small-sats, however, and have a more generous SWaP-C budget than what is feasible for nanosatellites, so achieving similar performance on a nanosatellite will prove challenging. A combination of radiation shielding, thermal annealing of the SPADs, adjusting the temperature, and managing over-voltage levels to maintain low dark count rates will remain the primary solution to defending against worsening detector efficiency due to the space environment. Demonstrated solutions for nanosatellites have been seen in the Galassia LEO nanosatellite, where the onboard detection system experienced a rapid increase in dark count rate, exceeding predictive models, after only 36 days [36]. A control circuit managed the operating voltage to counteract worsening performance, but it was suggested that the aluminium housing that provided radiation shielding needed to be thicker to be effective [36]. Unfortunately for a nanosatellite platform, all of the mitigation techniques, apart from annealing, typically require ample volume, mass and power.

Fig. 6 presents some suggested improvements to satellite detection systems.

2) HOMODYNE DETECTION SYSTEM CHALLENGES

Homodyne detection performance for quantum communications is typically dependent on bandwidth, detection efficiency, electric noise and Quantum-to-Classical Noise Ratio (QCNR). Bandwidth limits the multiplexing and processing of quantum signals and auxiliary classical signals (LO or pilot tone). Electronic noise reduces the SNR, and the QCNR is a measure of how well the weak quantum signal is amplified while suppressing electrical noise; generally required to be at least 10 dB [3]. The limitations of current

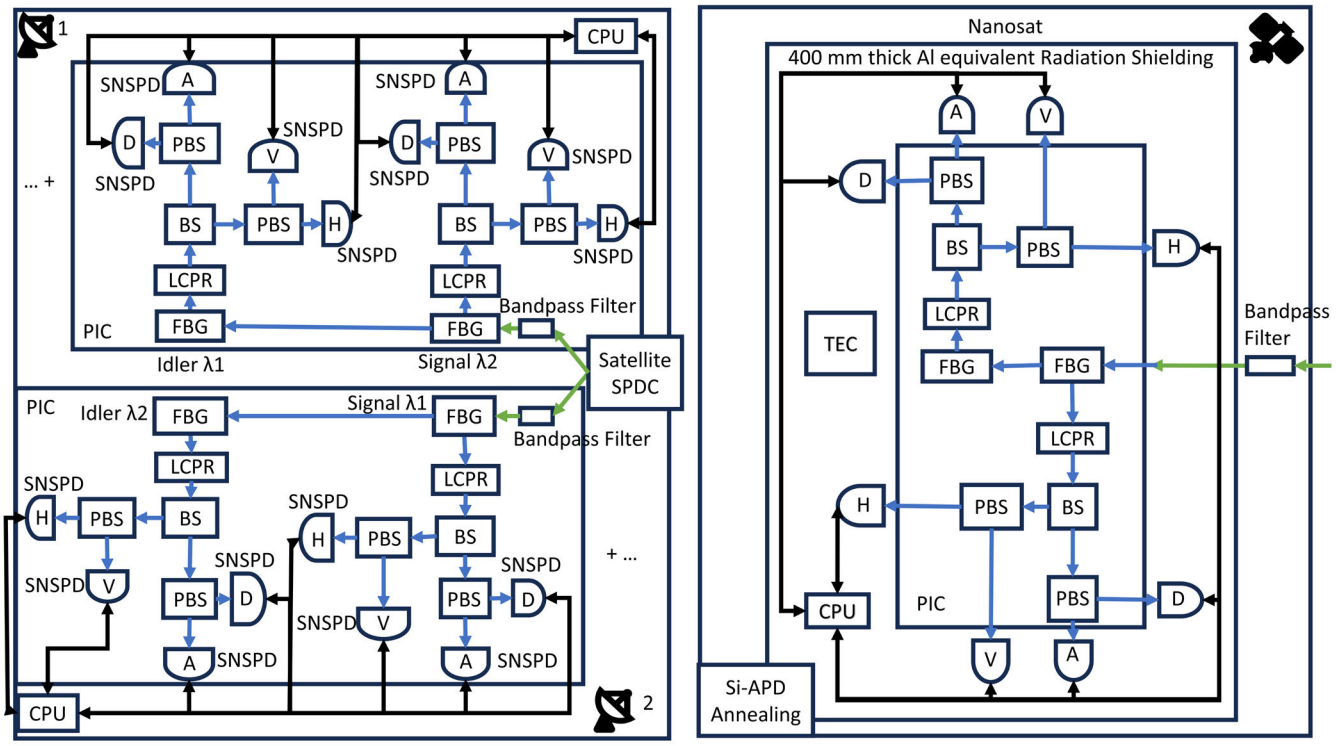

FIGURE 6. Suggested improvements of detection systems for OGSs and satellites. The Schematic is based on polarisation-entangled DV-QKD. The quantum signal is denoted by green. Power/Data lines are denoted by black. Dark blue denotes optical fibre. PBS: polarising beamsplitter. BS: beamsplitter. FBG: fibre Bragg grating. TEC: thermoelectric cooling. PIC: photonic integrated circuit. LCPR: liquid crystal polarisation rotator.

coherent detection systems require the average power of the transmitted signal to be adjusted (typically with a variable optical attenuator) to around several photons, as they are unable to correctly measure quantum characteristics of high-power quantum states.

A TLO scheme has the advantage of both the reference and modulated signal undergoing the same phase and polarisation changes that occur when subject to atmospheric effects in downlink/uplink configuration, making it easier to accurately compensate for these effects, as the phase mismatch will be less than a LLO scheme. It does, however, suffer vulnerability from a security perspective [3], [70]; more specifically, it is vulnerable to side-channel attacks [8]. Unfortunately, while the TLO scheme has the advantage of reducing phase mismatch during transmission through the atmosphere, it also has a distinct disadvantage of a potentially weak local oscillator signal due to loss in the channel; when attenuation is considerable, it can render the local oscillator signal power insufficient for homodyne detection.

LLO schemes solve the security issues of a TLO scheme by removing access to the LO from a third-party eavesdropper and thus removing the possibility of a side channel attack completely [8], [70]. This is at the expense of increased phase mismatch between the LO and the modulated signal when compared to TLO schemes. Demonstrations with a theoretical model have shown that an LLO scheme may suffer slight performance degradation in comparison to a TLO scheme under a satellite downlink channel [70]. The rectification of the frequency and phase mismatch presents a significant challenge for LLO schemes, and DSP is often used as a solution.

DSP can be used to compensate for several effects of channel corruption of the signal, and can often replace analogue equipment that would otherwise have compensated for the corruption. This can be useful where volume may be restricted; however, DSP algorithms can be very computationally intensive, requiring large power draws and creating thermal variations. Coherent receivers on-board nanosatellites also have to contend with the Doppler shift of the signal, which requires extra DSP blocks to compensate for it, and thus has sparked research into replacing DSP with analogue counterparts like OIPLL [75], [76]. As discussed in Section I-C, the Doppler shift presents a significant problem for coherent satellite communications, both classical and quantum. DSP algorithms can be used to compensate for the Doppler shift, but carrier recovery algorithms need to have a bandwidth large enough to accommodate the full Doppler shift range [75]. In general, DSP can offer flexibility and fewer constraints on analogue components, which has made it a critical component of current coherent detection systems. Improvements to algorithm efficiency and speed, paired with hardware designed for fast computations (FPGAs), will continue to improve the value proposition of digital signal

processing for both classical and quantum LEO nanosatellite communications.

There has been success in classical coherent optical nanosatellite communications from missions like NASA's TBIRD [18], [77], [78], whose success was enabled by advances in DSP. Due to comoninality in hardware, there is a natural compatibility for some DSP algorithms that can be applied for both classical and quantum coherent communications, EAGLE-1 is a promising upcoming mission that will use a BB84 decoy protocol with relative phase encoding for QKD at 1550 nm, and a coherent detection system using hardware found in classical coherent optical communications [79]. Aspects of success in one field should apply to the other, so future quantum communications LEO nanosatellite CV-QKD systems may be possible.

CV-QKD protocols require error correction and parameter estimation to be extremely accurate, as the verifiable security of the link is dependent on them. It is typically computationally expensive to perform these algorithms, and parameter estimation is considered the main bottleneck for extending CV-QKD to large distances [8]. To claim security, finite size effects need to be reduced, which often increases data block size, which is typically proportional to distance [8]. In turn, requires higher clock rates and detectors with larger bandwidths.

V. CONCLUSION

This review has explored the current state of the art for ATP systems, receiver systems and detection systems for LEO nanosatellite quantum communications.

Nanosatellites provide the optimal path towards a quantum internet constellation at LEO, providing a good balance between affordability and reliability, and this is echoed in the general trend towards nanosatellite missions within the field. As discussed, either LEO or GEO is the preferred orbit selection: LEO for the short distance between transmitter and receiver, and GEO for continuous coverage and operation. LEO nanosatellites are easy and low-cost to launch via a ride-share, they are inexpensive to produce, and although they tend to require a higher replenishment rate (due to component degradation) than micro or small satellites, this can be used for faster innovation cycles.

From the analysis of the ATP systems deployed by [30], [31], [32], and [34], a two-way beacon system provides a promising solution to the high precision tracking required for increasing the quantum signal-to-noise ratio. There are still optimisations that could be made, from improving the detection and tracking algorithms [35] to improvements in point ahead mechanisms or algorithms [31].

Receiver and detector efficiencies of on-board receiver and detection systems have been maximised with radiation shielding and through control of temperature and voltage [47], [54] and through demultiplexing schemes to increase the number of communication channels in the system [69], [80]. Si-SPADs represent the most popular single photon detectors for receivers and detection systems on-board nanosatellite platforms, due to their maturity and low volume and mass. Improvements to detection technologies, such as a new substrate instead of Silicon that produces a higher detection efficiency for quantum signal wavelengths or the development of SNSPDs that can operate in non-cryogenic environments, may challenge the dominance of Si-SPADs in LEO nanosatellite quantum communications receivers and detection systems.

Ground station receivers and detection systems have also used Si-SPADs, but new and upcoming missions are moving towards SNSPDs, connected by single-mode fibre to adaptive optics systems that couple them to the free space quantum signal [19]. This trend is likely to continue as the performance offered by SNSPDs is much greater than SPADs, and ground facilities are much better equipped to handle the current cryogenic requirements. However, a low-cost option for an OGS may still opt for SPADs as their detection system, as the equipment requirements are less than SNSPDs, which require both adaptive optics and cryogenic cooling systems.

Homodyne and heterodyne detectors are still under-represented in practical demonstrations of CV-QKD over satellite quantum communications and require much more work in improving and optimising the efficiencies of their associated DSP algorithms.

Miniaturisation remains a significant challenge for LEO nanosatellite quantum communications receivers and detection systems, as many components and strategies seen in larger satellites do not scale down intuitively.

Daylight operations will enable a much more responsive QKD network and warrant more work to support it. Stricter filtering of background light and faster spot detection and tracking algorithms may enable daytime operational capabilities, but coherent detection systems have been proven to work during daytime conditions.

Ultimately, improving upon the performance of the ATP, receiver, and detection systems will increase the feasibility of a global satellite quantum communications network and pave the way towards a quantum internet.

REFERENCES

[1] J. S. Sidhu, S. K. Joshi, M. Gündoğan, T. Brougham, D. Lowndes, L. Mazzarella, M. Krutzik, S. R. P. Mohapatra, D. Dequal, G. Vallone, P. Villoresi, A. Ling, T. Jennewein, M. Mohageg, J. Rarity, I. Fuentes, S. Pirandola, and D. K. L. Oi, "Advances in space quantum communications," *IET Quantum Commun.*, vol. 2, no. 4, pp. 182–217, 2021.

[2] R. Bedington, J. M. Arrazola, and A. Ling, "Progress in satellite quantum key distribution," *npj Quantum Inf.*, vol. 3, no. 1, p. 30, Aug. 2017, doi: 10.1038/s41534-017-0031-5.

[3] Y. Zhang, Y. Bian, Z. Li, S. Yu, and H. Guo, "Continuous-variable quantum key distribution system: Past, present, and future," *Appl. Phys. Rev.*, vol. 11, no. 1, Mar. 2024, Art. no. 011318, doi: 10.1063/5.0179566.

[4] T. Islam, J. S. Sidhu, B. L. Higgins, T. Brougham, T. Vergoossen, D. K. L. Oi, T. Jennewein, and A. Ling, "Finite-resource performance of small-satellite-based quantum-key-distribution missions," *PRX Quantum*, vol. 5, no. 3, Jul. 2024, Art. no. 030101. [Online]. Available: https://link.aps.org/doi/10.1103/PRXQuantum.5.030101

[5] J. Yin et al., "Satellite-based entanglement distribution over 1200 kilometers," *Science*, vol. 356, no. 6343, pp. 1140–1144, Jun. 2017. [Online]. Available: https://www.science.org/doi/abs/10.1126/science.aan3211

[6] Y. Shoji, M. J. Fice, Y. Takayama, and A. J. Seeds, "A pilot-carrier coherent LEO-to-ground downlink system using an optical injection phase lock loop (OIPLL) technique," *J. Lightw. Technol.*, vol. 30, no. 16, pp. 2696–2706, Aug. 15, 2012, doi: 10.1109/JLT.2012.2204037. [Online]. Available: https://opg.optica.org/jlt/abstract.cfm?URI=jlt-30-16-2696

[7] L. B. Stotts, *Optical Channel Effects*. Hoboken, NJ, USA: Wiley, 2017, pp. 239–298. [Online]. Available: https://onlinelibrary.wiley.com/doi/abs/10.1002/9781119279068.ch7

[8] S. Pirandola, U. L. Andersen, L. Banchi, M. Berta, D. Bunandar, R. Colbeck, D. Englund, T. Gehring, C. Lupo, C. Ottaviani, J. L. Pereira, M. Razavi, J. S. Shaari, M. Tomamichel, V. C. Usenko, G. Vallone, P. Villoresi, and P. Wallden, "Advances in quantum cryptography," *Adv. Opt. Photon.*, vol. 12, no. 4, p. 1012, 2020.

[9] S. Pirandola, R. Laurenza, C. Ottaviani, and L. Banchi, "Fundamental limits of repeaterless quantum communications," *Nature Commun.*, vol. 8, no. 1, p. 15043, Apr. 2017, doi: 10.1038/ncomms15043.

[10] S. Pirandola, R. García-Patrón, S. L. Braunstein, and S. Lloyd, "Direct and reverse secret-key capacities of a quantum channel," *Phys. Rev. Lett.*, vol. 102, no. 5, Feb. 2009, Art. no. 050503. [Online]. Available: https://link.aps.org/doi/10.1103/PhysRevLett.102.050503

[11] S. Pirandola, "Satellite quantum communications: Fundamental bounds and practical security," *Phys. Rev. Res.*, vol. 3, no. 2, May 2021, Art. no. 023130. [Online]. Available: https://link.aps.org/doi/10.1103/PhysRevResearch.3.023130

[12] B. Dirks, I. Ferrario, A. L. Pera, D. Finocchiaro, M. Desmons, D. D. Lange, H. D. Man, A. J. H. Meskers, J. Morits, N. M. P. Neumann, R. Saathof, and G. Witvoet, "GEOQKD: Quantum key distribution from a geostationary satellite," *Proc. SPIE*, vol. 11852, May 2021, Art. no. 118520J, doi: 10.1117/12.2599164.

[13] M. T. Gruneisen, M. L. Eickhoff, S. C. Newey, K. E. Stoltenberg, J. F. Morris, M. Bareian, M. A. Harris, D. W. Oesch, M. D. Oliker, M. B. Flanagan, B. T. Kay, J. D. Schiller, and R. N. Lanning, "Adaptive-optics-enabled quantum communication: A technique for daytime space-to-Earth links," *Phys. Rev. Appl.*, vol. 16, no. 1, Jul. 2021, Art. no. 014067. [Online]. Available: https://link.aps.org/doi/10.1103/PhysRevApplied.16.014067

[14] N. Martinez, "Atmospheric pre-compensation of ground-to-space communications with adaptive optics: Past, present and future—A field review," *Photonics*, vol. 10, no. 7, p. 858, Jul. 2023. [Online]. Available: https://www.mdpi.com/2304-6732/10/7/858

[15] C. Fuchs, F. Moll, J. Poliak, A. Reeves, and C. Schmidt, "Optical satellite links for telecommunications and time-transfer," in *Proc. IEEE Int. Conf. Space Opt. Syst. Appl. (ICSOS)*, Oct. 2023, pp. 168–174.

[16] C. J. Pugh, J.-F. Lavigne, J.-P. Bourgoin, B. L. Higgins, and T. Jennewein, "Adaptive optics benefit for quantum key distribution uplink from ground to a satellite," *Adv. Opt. Technol.*, vol. 9, no. 5, pp. 263–273, Nov. 2020, doi: 10.1515/aot-2020-0017.

[17] L. Scarfe, F. Hufnagel, M. F. Ferrer-Garcia, A. D'Errico, K. Heshami, and E. Karimi, "Fast adaptive optics for high-dimensional quantum communications in turbulent channels," *Commun. Phys.*, vol. 8, no. 1, p. 79, Feb. 2025, doi: 10.1038/s42005-025-01986-6.

[18] C. Schieler, K. Riesing, B. Bilyeu, J. S. Chang, A. S. Garg, N. C. Gilbert, A. Horváth, R. Reeve, B. S. Robinson, J. P. Wang, S. Piazzolla, W. T. Roberts, J. Kovalik, and B. Keer, "On-orbit demonstration of 200-gbps laser communication downlink from the TBIRD CubeSat," *Proc. SPIE*, vol. 12413, Mar. 2023, Art. no. 1241302, doi: 10.1117/12.2651297.

[19] M. Jagnji, J. Vukovi, B. Skendrovi, J. Lonar, M. Lonari, and D. Babi, "Optical ground station proposal for croatian quantum communication infrastructure," in *Proc. 47th MIPRO ICT Electron. Conv. (MIPRO)*, May 2024, pp. 1721–1726.

[20] M. Chen, C. Liu, D. Rui, and H. Xian, "Performance verification of adaptive optics for satellite-to-ground coherent optical communications at large zenith angle," *Opt. Exp.*, vol. 26, no. 4, pp. 4230–4242, 2018. [Online]. Available: https://opg.optica.org/oe/abstract.cfm?URI=oe-26-4-4230

[21] Y. Wang, H. Xu, D. Li, R. Wang, C. Jin, X. Yin, S. Gao, Q. Mu, L. Xuan, and Z. Cao, "Performance analysis of an adaptive optics system for free-space optics communication through atmospheric turbulence," *Sci. Rep.*, vol. 8, no. 1, p. 1124, Jan. 2018, doi: 10.1038/s41598-018-19559-9.

[22] L. Yang, K. Yao, J. Wang, J. Cao, X. Lin, X. Liu, W. Liu, and H. Gu, "Performance analysis of 349-element adaptive optics unit for a coherent free space optical communication system," *Sci. Rep.*, vol. 9, no. 1, p. 13150, Sep. 2019, doi: 10.1038/s41598-019-48338-3.

[23] K. S. Chan and H. F. Chau, "Reducing the impact of adaptive optics lag on optical and quantum communications rates from rapidly moving sources," *AIP Adv.*, vol. 13, no. 5, May 2023, Art. no. 055201, doi: 10.1063/5.0149695.

[24] P. Parvizi, R. Zou, C. Bellinger, R. Cheriton, and D. Spinello, "Reinforcement learning environment for wavefront sensorless adaptive optics in single-mode fiber coupled optical satellite communications downlinks," *Photonics*, vol. 10, no. 12, p. 1371, Dec. 2023. [Online]. Available: https://www.mdpi.com/2304-6732/10/12/1371

[25] D. Giggenbach, C. Fuchs, C. Schmidt, B. Rödiger, S. Gaißer, S. Klinkner, D.-H. Phung, J. Chabé, C. Courde, N. Maurice, H. Mariey, E. Samain, and G. Artaud, "Downlink communication experiments with OSIRISv1 laser terminal onboard flying laptop satellite," *Appl. Opt.*, vol. 61, no. 8, pp. 1938–1946, 2022. [Online]. Available: https://opg.optica.org/ao/abstract.cfm?URI=ao-61-8-1938

[26] C. Fuchs, C. Schmidt, J. Keim, F. Moll, B. Rödiger, M. Lengowski, S. Gaißer, and D. Giggenbach, "Update on DLR's OSIRIS program and first results of OSIRISv1 on flying laptop," *Proc. SPIE*, vol. 10910, Mar. 2019, Art. no. 109100S, doi: 10.1117/12.2514349.

[27] B. Rödiger, C. Menninger, C. Fuchs, L. Grillmayer, S. Arnold, C. Rochow, P. Wertz, and C. C. Schmidt, "High data-rate optical communication payload for CubeSats," *Proc. SPIE*, vol. 11506, p. 3, Jan. 2020, Art. no. 1150604, doi: 10.1117/12.2567035.

[28] B. Rödiger, M.-T. Hahn, C. Fuchs, and C. C. Schmidt, "OSIRIS4CubeSat–system engineering with new space approach from the development of a high data-rate optical communication payload to the demonstrator in a quasi-operational mission," in *Proc. 9th Int. Syst. Concurrent Eng. Space Appl. Conf.*, Dec. 2020, pp. 1–16. [Online]. Available: https://elib.dlr.de/136602/

[29] A. V. Miller, L. V. Pismeniuk, A. V. Duplinsky, V. E. Merzlinkin, A. A. Plukchi, K. A. Tikhonova, I. S. Nesterov, D. O. Sevryukov, S. D. Levashov, V. V. Fetisov, S. V. Krasnopejev, and R. M. Bakhshaliev, "Vector—Towards quantum key distribution with small satellites," *EPJ Quantum Technol.*, vol. 10, no. 1, p. 52, 2023.

[30] A. V. Khmelev, A. V. Duplinsky, V. L. Kurochkin, and Y. V. Kurochkin, "Stellar calibration of the single-photon receiver for satellite-to-ground quantum key distribution," *J. Phys., Conf. Ser.*, vol. 2086, no. 1, Dec. 2021, Art. no. 012137, doi: 10.1088/1742-6596/2086/1/012137.

[31] L. Zhang, J. Dai, C. Li, J. Wu, J. Jia, and J. Wang, "Design and in-orbit test of a high accuracy pointing method in satellite-to-ground quantum communication," *Opt. Exp.*, vol. 28, no. 6, pp. 8291–8307, 2020. [Online]. Available: https://opg.optica.org/oe/abstract.cfm?URI=oe-28-6-8291

[32] C. J. Pugh, S. Kaiser, J.-P. Bourgoin, J. Jin, N. Sultana, S. Agne, E. Anisimova, V. Makarov, E. Choi, B. L. Higgins, and T. Jennewein, "Airborne demonstration of a quantum key distribution receiver payload," *Quantum Sci. Technol.*, vol. 2, no. 2, Jun. 2017, Art. no. 024009, doi: 10.1088/2058-9565/aa701f.

[33] M. Birch, N. Martínez, F. Bennet, M. Copeland, and D. Grosse, "The mount stromlo optical communication ground station," in *Proc. IEEE Int. Conf. Space Opt. Syst. Appl. (ICSOS)*, Mar. 2022, pp. 134–137.

[34] C. D. Colquhoun, "Responsive operations for key services (roks) : A modular, low swap quantum communications payload," in *Proc. AIAA/USU Conf. Small Satell.*, Oct. 2022, pp. 1–13. [Online]. Available: https://strathprints.strath.ac.uk/85639/

[35] Q. Wang, X. Wang, L. Cui, L. Tan, and J. Ma, "Approach of recognition and precision location for the beacon in satellite optical communications," *Optik*, vol. 260, Jun. 2022, Art. no. 169091. [Online]. Available: https://www.sciencedirect.com/science/article/pii/S0030402622004570

[36] Z. Tang, R. Chandrasekara, Y. C. Tan, C. Cheng, L. Sha, G. C. Hiang, D. K. L. Oi, and A. Ling, "Generation and analysis of correlated pairs of photons aboard a nanosatellite," *Phys. Rev. Appl.*, vol. 5, no. 5, May 2016, Art. no. 054022, doi: 10.1103/PhysRevApplied.5.054022.

[37] A. Lohrmann, C. Perumgatt, and A. Ling, "Manipulation and measurement of quantum states with liquid crystal devices," *Opt. Exp.*, vol. 27, no. 10, pp. 13765–13772, 2019. [Online]. Available: https://opg.optica.org/oe/abstract.cfm?URI=oe-27-10-13765

[38] A. Villar, A. Lohrmann, X. Bai, T. Vergoossen, R. Bedington, C. Perumangatt, H. Y. Lim, T. Islam, A. Reezwana, Z. Tang, R. Chandrasekara, S. Sachidananda, K. Durak, C. F. Wildfeuer, D. Griffin, D. K. L. Oi, and A. Ling, "Entanglement demonstration on board a nano-satellite," *Optica*, vol. 7, no. 7, p. 734, 2020.

[39] H. Kaushal, V. K. Jain, and S. Kar, *FSO System Modules and Design Issues*. New Delhi, India: Springer, 2017, pp. 91–118, doi: 10.1007/978-81-322-3691-7_3.

[40] O. Pryce-Jones, S. Fowler, R. Davies, A. Tringali, L. Foley, S. Mardhani, D. O'Connell, A. Harpin, N. Shanmugasundaram, T. W. Hussey, J. Nygaard, J. Alston, C. Quintana, and E. Fiamanya, "Testing a small, deployable, optical ground terminal for LEO to ground laser communications," *Proc. SPIE*, vol. 13355, Jun. 2025, Art. no. 133552B, doi: 10.1117/12.3047990.

[41] L. Mazzarella, C. Lowe, D. Lowndes, S. K. Joshi, S. Greenland, D. McNeil, C. Mercury, M. Macdonald, J. Rarity, and D. K. L. Oi, "QUARC: Quantum research cubesat—A constellation for quantum communication," *Cryptography*, vol. 4, no. 1, p. 7, Feb. 2020. [Online]. Available: https://www.mdpi.com/2410-387X/4/1/7

[42] J.-G. Ren et al., "Ground-to-satellite quantum teleportation," *Nature*, vol. 549, no. 7670, pp. 70–73, 2017.

[43] S. Hearne, J. Horgan, N. Boujnah, and D. Kilbane, "Wavelength selection for satellite quantum key distribution," *Appl. Sci.*, vol. 15, no. 3, p. 1308, Jan. 2025. [Online]. Available: https://www.mdpi.com/2076-3417/15/3/1308

[44] D. Garoli, L. V. Rodriguez De Marcos, J. I. Larruquert, A. J. Corso, R. P. Zaccaria, and M. G. Pelizzo, "Mirrors for space telescopes: Degradation issues," *Appl. Sci.*, vol. 10, no. 21, p. 7538, Oct. 2020. [Online]. Available: https://www.mdpi.com/2076-3417/10/21/7538

[45] P. B. Johnson and R. W. Christy, "Optical constants of the noble metals," *Phys. Rev. B, Condens. Matter*, vol. 6, no. 12, pp. 4370–4379, Dec. 1972. [Online]. Available: https://link.aps.org/doi/10.1103/PhysRevB.6.4370

[46] A. D. Rakić, "Algorithm for the determination of intrinsic optical constants of metal films: Application to aluminum," *Appl. Opt.*, vol. 34, no. 22, pp. 4755–4767, 1995. [Online]. Available: https://opg.optica.org/ao/abstract.cfm?URI=ao-34-22-4755

[47] N. Ahmadi et al., "QUICK^3—Design of a satellite-based quantum light source for quantum communication and extended physical theory tests in space," *Adv. Quantum Technol.*, vol. 7, no. 4, Apr. 2024, Art. no. 2300343. [Online]. Available: https://advanced.onlinelibrary.wiley.com/doi/abs/10.1002/qute.202300343

[48] J. Osborn, M. J. Townson, O. J. D. Farley, A. Reeves, and R. M. Calvo, "Adaptive optics pre-compensated laser uplink to LEO and GEO," *Opt. Exp.*, vol. 29, no. 4, pp. 6113–6132, Feb. 2021. [Online]. Available: https://opg.optica.org/oe/abstract.cfm?URI=oe-29-4-6113

[49] A. Berk, P. Conforti, R. Kennett, T. Perkins, F. Hawes, and J. van den Bosch, "MODTRAN 6: A major upgrade of the MODTRAN radiative transfer code," in *Proc. 6th Workshop Hyperspectral Image Signal Process., Evol. Remote Sens.*, Jun. 2014, pp. 1–4.

[50] A. Berk, P. F. Conforti, and F. Hawes, "An accelerated line-by-line option for MODTRAN combining on-the-fly generation of line center absorption within 0.1 cm-1 bins and pre-computed line tails," *Proc. SPIE*, vol. 9472, Apr. 2015, Art. no. 947217, doi: 10.1117/12.2177444.

[51] C. Fuchs, M. Brechtelsbauer, J. Horwath, A. Shrestha, F. Moll, D. Giggenbach, and C. Schmidt, "Dlr's transportable optical ground station," in *Proc. Advanced Solid-State Lasers Congress*, 2013, pp. 1–3. [Online]. Available: https://opg.optica.org/abstract.cfm?URI=LSC-2013-LTu1B.3

[52] D. Vasylyev, W. Vogel, and F. Moll, "Satellite-mediated quantum atmospheric links," *Phys. Rev. A, Gen. Phys.*, vol. 99, no. 5, May 2019, Art. no. 053830. [Online]. Available: https://link.aps.org/doi/10.1103/PhysRevA.99.053830

[53] G. Vallone, D. Bacco, D. Dequal, S. Gaiarin, V. Luceri, G. Bianco, and P. Villoresi, "Experimental satellite quantum communications," *Phys. Rev. Lett.*, vol. 115, no. 4, Jul. 2015, Art. no. 040502, doi: 10.1103/PhysRevLett.115.040502.

[54] M. Yang, F. Xu, J.-G. Ren, J. Yin, Y. Li, Y. Cao, Q. Shen, H.-L. Yong, L. Zhang, S.-K. Liao, J.-W. Pan, and C.-Z. Peng, "Spaceborne, low-noise, single-photon detection for satellite-based quantum communications," *Opt. Exp.*, vol. 27, no. 25, p. 36114, 2019.

[55] H. Li, L. Zhang, L. You, X. Yang, W. Zhang, X. Liu, S. Chen, Z. Wang, and X. Xie, "Large-sensitive-area superconducting nanowire single-photon detector at 850 nm with high detection efficiency," *Opt. Exp.*, vol. 23, no. 13, pp. 17301–17308, 2015. [Online]. Available: https://opg.optica.org/oe/abstract.cfm?URI=oe-23-13-17301

[56] D. V. Reddy, R. R. Nerem, S. W. Nam, R. P. Mirin, and V. B. Verma, "Superconducting nanowire single-photon detectors with 98% system detection efficiency at 1550 nm," *Optica*, vol. 7, no. 12, p. 1649, 2020. [Online]. Available: https://opg.optica.org/optica/abstract.cfm?URI=optica-7-12-1649

[57] M. A. Wolff, F. Beutel, J. Schtte, H. Gehring, M. Huler, W. Pernice, and C. Schuck, "Broadband waveguide-integrated superconducting single-photon detectors with high system detection efficiency," *Appl. Phys. Lett.*, vol. 118, no. 15, Apr. 2021, Art. no. 154004, doi: 10.1063/5.0046057.

[58] G. G. Taylor, A. B. Walter, B. Korzh, B. Bumble, S. R. Patel, J. P. Allmaras, A. D. Beyer, R. O'Brient, M. D. Shaw, and E. E. Wollman, "Low-noise single-photon counting superconducting nanowire detectors at infrared wavelengths up to 29 μm," *Optica*, vol. 10, no. 12, pp. 1672–1678, 2023. [Online]. Available: https://opg.optica.org/optica/abstract.cfm?URI=optica-10-12-1672

[59] J. W. N. Los, M. Sidorova, B. Lopez-Rodriguez, P. Qualm, J. Chang, S. Steinhauer, V. Zwiller, and I. E. Zadeh, "High-performance photon number resolving detectors for 850–950 nm wavelength range," *APL Photon.*, vol. 9, no. 6, Jun. 2024, Art. no. 066101, doi: 10.1063/5.0204340.

[60] I. Esmaeil Zadeh, J. Chang, J. W. N. Los, S. Gyger, A. W. Elshaari, S. Steinhauer, S. N. Dorenbos, and V. Zwiller, "Superconducting nanowire single-photon detectors: A perspective on evolution, state-of-the-art, future developments, and applications," *Appl. Phys. Lett.*, vol. 118, no. 19, May 2021, Art. no. 190502, doi: 10.1063/5.0045990.

[61] Y. Pei, Q. Fan, X. Ni, and X. Gu, "Controlling the superconducting critical temperature and resistance of NbN films through thin film deposition and annealing," *Coatings*, vol. 14, no. 4, p. 496, Apr. 2024. [Online]. Available: https://www.mdpi.com/2079-6412/14/4/496

[62] I. Charaev, D. A. Bandurin, A. T. Bollinger, I. Y. Phinney, I. Drozdov, M. Colangelo, B. A. Butters, T. Taniguchi, K. Watanabe, X. He, O. Medeiros, I. Božović, P. Jarillo-Herrero, and K. K. Berggren, "Single-photon detection using high-temperature superconductors," *Nature Nanotechnol.*, vol. 18, no. 4, pp. 343–349, Apr. 2023, doi: 10.1038/s41565-023-01325-2.

[63] G. Xu, W. Zhang, L. You, J.-M. Xiong, X.-Q. Sun, H. Huang, X. Ou, Y. Pan, C. Lv, H. Li, Z. Wang, and X. Xie, "Superconducting microstrip single-photon detector with system detection efficiency over 90% at 1550 nm," *Photon. Res.*, vol. 9, no. 6, p. 958, 2021. [Online]. Available: https://opg.optica.org/prj/abstract.cfm?URI=prj-9-6-958

[64] G.-Z. Xu, W.-J. Zhang, L.-X. You, Y.-Z. Wang, J.-M. Xiong, D.-H. Fan, L. Wu, H.-Q. Yu, H. Li, and Z. Wang, "Millimeter-scale active area superconducting microstrip single-photon detector fabricated by ultraviolet photolithography," *Opt. Exp.*, vol. 31, no. 10, pp. 16348–16360, 2023. [Online]. Available: https://opg.optica.org/oe/abstract.cfm?URI=oe-31-10-16348

[65] Y.-Z. Wang, W.-J. Zhang, X.-Y. Zhang, G.-Z. Xu, J.-M. Xiong, Z.-G. Chen, Y.-Y. Hong, X.-Y. Liu, P.-S. Yuan, L. Wu, Z. Wang, and L.-X. You, "Free-space coupled, large-active-area superconducting microstrip single-photon detector for photon-counting time-of-flight imaging," *Appl. Opt.*, vol. 63, no. 12, pp. 3130–3137, 2024. [Online]. Available: https://opg.optica.org/ao/abstract.cfm?URI=ao-63-12-3130

[66] L.-D. Kong, H. Wang, Q.-Y. Zhao, J.-W. Guo, Y.-H. Huang, H. Hao, S. Chen, X.-C. Tu, L.-B. Zhang, X.-Q. Jia, L. Kang, J. Chen, and P.-H. Wu, "Readout-efficient superconducting nanowire single-photon imager with orthogonal time–amplitude multiplexing by hotspot quantization," *Nature Photon.*, vol. 17, no. 1, pp. 65–72, Jan. 2023, doi: 10.1038/s41566-022-01089-6.

[67] E. E. Wollman, V. B. Verma, A. E. Lita, W. H. Farr, M. D. Shaw, R. P. Mirin, and S. Woo Nam, "Kilopixel array of superconducting nanowire single-photon detectors," *Opt. Exp.*, vol. 27, no. 24, pp. 35279–35289, 2019. [Online]. Available: https://opg.optica.org/oe/abstract.cfm?URI=oe-27-24-35279

[68] S. Saravi, T. Pertsch, and F. Setzpfandt, "Lithium niobate on insulator: An emerging platform for integrated quantum photonics," *Adv. Opt. Mater.*, vol. 9, no. 22, Nov. 2021, Art. no. 2100789. [Online]. Available: https://onlinelibrary.wiley.com/doi/abs/10.1002/adom.202100789

[69] E. Brambila, R. Gómez, R. Fazili, M. Gräfe, and F. Steinlechner, "Ultrabright polarization-entangled photon pair source for frequency-multiplexed quantum communication in free-space," *Opt. Exp.*, vol. 31, no. 10, pp. 16107–16117, 2023. [Online]. Available: https://opg.optica.org/oe/abstract.cfm?URI=oe-31-10-16107

[70] S. P. Kish, E. Villaseñor, R. Malaney, K. A. Mudge, and K. J. Grant, "Use of a local local oscillator for the satellite-to-Earth channel," in *Proc. IEEE Int. Conf. Commun.*, Jun. 2021, pp. 1–6.

[71] K. Günthner, I. Khan, D. Elser, B. Stiller, Ö. Bayraktar, C. R. Müller, K. Saucke, D. Tröndle, F. Heine, S. Seel, P. Greulich, H. Zech, B. Gütlich, S. Philipp-May, C. Marquardt, and G. Leuchs, "Quantum-limited measurements of optical signals from a geostationary satellite," *Optica*, vol. 4, no. 6, pp. 611–616, Jun. 2017. [Online]. Available: https://opg.optica.org/optica/abstract.cfm?URI=optica-4-6-611

[72] J. S. Sidhu, T. Brougham, D. McArthur, R. G. Pousa, and D. K. L. Oi, "Finite key effects in satellite quantum key distribution," *npj Quantum Inf.*, vol. 8, no. 1, pp. 2056–6387, Feb. 2022, doi: 10.1038/s41534-022-00525-3.

[73] R. N. Lanning, M. A. Harris, D. W. Oesch, M. D. Oliker, and M. T. Gruneisen, "Quantum communication over atmospheric channels: A framework for optimizing wavelength and filtering," *Phys. Rev. Appl.*, vol. 16, no. 4, Oct. 2021, Art. no. 044027. [Online]. Available: https://link.aps.org/doi/10.1103/PhysRevApplied.16.044027

[74] H. Ko, K.-J. Kim, J.-S. Choe, B.-S. Choi, J.-H. Kim, Y. Baek, and C. J. Youn, "Experimental filtering effect on the daylight operation of a free-space quantum key distribution," *Sci. Rep.*, vol. 8, no. 1, p. 15315, Oct. 2018, doi: 10.1038/s41598-018-33699-y.

[75] A. W. Bernini, M. J. Fice, and K. Balakier, "Low-power-consumption coherent receiver architecture for satellite optical links," in *Proc. IEEE Int. Conf. Space Opt. Syst. Appl. (ICSOS)*, Mar. 2022, pp. 149–153.

[76] A. W. Bernini, M. J. Fice, and K. Balakier, "Phase locking of an optical injection phase-lock loop coherent receiver under emulated atmospheric fading conditions," in *Proc. Opt. Fiber Commun. Conf. Exhib. (OFC)*, Mar. 2023, pp. 1–3.

[77] S. M. Walsh, S. F. E. Karpathakis, A. S. McCann, B. P. Dix-Matthews, A. M. Frost, D. R. Gozzard, C. T. Gravestock, and S. W. Schediwy, "Demonstration of 100 Gbps coherent free-space optical communications at LEO tracking rates," *Sci. Rep.*, vol. 12, no. 1, p. 18345, Oct. 2022, doi: 10.1038/s41598-022-22027-0.

[78] C. Schieler, K. Riesing, A. Horváth, B. Bilyeu, J. Chang, A. S. Garg, J. P. Wang, and B. S. Robinson, "200 Gbps TBIRD CubeSat downlink: Pre-flight test results," *Proc. SPIE*, vol. 11993, Jun. 2022, Art. no. 119930P, doi: 10.1117/12.2615321.

[79] G. Calistro Rivera, O. Heirich, A. Shrestha, A. Ferenczi, A. Duliu, J. Eppinger, B. Femenia Castella, C. Fuchs, E. Garbagnati, D. Laidlaw, P. Lützen, I. De Marco, F. Moll, J. Prell, J. Rosano Nonay, C. Roubal, J. Torres, and M. Wagner, "Building Europe's first space-based QKD system—The German aerospace center's role in the EAGLE-1 project," in *Proc. IAF Space Commun. Navigat. Symp.*, Nov. 2024, pp. 880–887. [Online]. Available: https://elib.dlr.de/208771/

[80] K. C. Chen, P. Dhara, M. Heuck, Y. Lee, W. Dai, S. Guha, and D. Englund, "Zero-added-loss entangled-photon multiplexing for ground- and space-based quantum networks," *Phys. Rev. Appl.*, vol. 19, no. 5, May 2023, Art. no. 054029. [Online]. Available: https://link.aps.org/doi/10.1103/PhysRevApplied.19.054029

JAMES J. SHAWE received the Bachelor of Science degree in physics with astronomy and space science from University College Dublin, Ireland, and the Master of Science degree in astronautics and space engineering from Cranfield University, U.K. He is currently pursuing the structured Ph.D. degree with the Department of Computing and Mathematics, South East Technological University, Ireland. He is currently a Doctoral Researcher with the Walton Institute for Information and Communication Systems Science, South East Technological University. Previously, he was with industry as a Space System and Satellite Operations Engineer with Aistech Space, Spain. His current research interests include satellite communications and quantum communications, with a focus on ground station infrastructure.

JERRY HORGAN received the Bachelor of Science degree in applied computing and the Master of Science degree in communications software from Waterford Institute of Technology, Ireland, and the Master of Science degree in IT and management from the National University of Ireland in Maynooth. He is a Lecturer with the Department of Computing and Mathematics and a Research Affiliate with the Walton Institute for Information and Communication Systems Science, South East Technological University, Ireland. His current research interests include satellite communications, quantum communications, security, and software defined infrastructure.

DEIRDRE KILBANE received the Bachelor of Science degree in experimental physics from University College Dublin, Ireland, and the Ph.D. degree in mathematical physics from the National University of Ireland in Maynooth. She is currently the Director of Research with the Walton Institute for Information and Communication Systems Science, South East Technological University, Ireland. Previously, she was a Marie Curie Fellow with the University of Kaiserslautern, Germany. She was a recipient of two Science Foundation Ireland Industry fellowships. She has authored or co-authored over 50 journal and conference papers and is a reviewer of many journals. Her current research interests include artificial intelligence, nano-optics, biosensing, and quantum communication.